Autoimmune encephalitis: Analysis of the intrathecal plasma cell repertoire and expression of patient derived antineuronal antibodies in recombinant form

Inaugural dissertation

for the attainment of the title of doctor
in the Faculty of Mathematics and Natural Sciences

at the Heinrich-Heine-University Düsseldorf

presented by

Manish Malviya

from Bhadohi, India

Düsseldorf, December 2014

from the Department of Neurology,

Heinrich-Heine-University Düsseldorf

Published by permission of the
Faculty of Mathematics and Natural Sciences,

Heinrich Heine University Düsseldorf

Supervisor: **Prof. Dr. Norbert Goebels**

Co-supervisor: **Prof. Dr. Dieter Willbold**

Date of the oral examination: _ _ /_ _ /2015

CONTENTS **Page No.**

CONTENTS.. **Page No.**

SUMMARY

The autoimmune encephalitis (AIE) syndromes are a recently identified group of conditions associated with autoantibodies specific for neuronal cell-surface or synaptic proteins. Previous studies of cerebrospinal fluid (CSF) and serum of patients with AIE have described the presence of antineuronal autoantibodies specific for the NMDA receptor, AMPA receptor, leucine-rich glioma inactivated protein 1 (LGI1), contactin-associated protein-like 2 (CASPR2), glutamic acid decarboxylase (GAD_{65}) and others. To investigate the origin and function of intrathecal autoantibodies in AIE patients, we aimed to examine the $CD138^{+}$ plasma cell repertoire and to reconstruct some of the antineuronal autoantibodies in the form of recombinant human monoclonal antibodies (rhuMAb).

After FACS sorting, we analysed 584 individual CSF plasma cells from five AIE patients by single cell RT-PCR, yielding 508 *immunoglobulin* heavy chain sequences. By analysis of the CDR3-sequence we detected clonally expanded plasma cells (cePc) in every examined CSF sample and identified a total of 57 independent plasma cell clones. We also analysed the relative representation of immunoglobulin germline families: A patient prediagnosed with anti-LGI1 autoantibodies (GKD) had a clear overrepresentation of the V_H4 family. The V_H1 family was underrepresented in a patient with anti-NMDA receptor autoantibodies (SSM). Two patients with anti-CASPR2 autoantibodies (KKM & BRM) had similar patterns of germline gene family representation in order of $V_H3>V_H1>V_H4>V_H5$. One of the patients with anti-CASPR2 autoantibodies also represented V_H7 family. The V_H1 family was mostly represented in a patient prediagnosed with anti-GAD_{65} (JMB) autoantibodies.

To elucidate whether cePc are the actual source of the intrathecal autantibody response, we successfully cloned and expressed paired immunoglobulin heavy and light chain genes from 16 cePc and one nonexpanded plasma cell from three of the five patients. Seven rhuMAb (SSM1-7) were reconstructed from a patient diagnosed with anti-NMDA receptor encephalitis; another seven antibodies (GKD1-7) were reproduced from a patient diagnosed with anti-LGI1 encephalitis; and three rhuMAb (JMB1-3) were made from a patient diagnosed with anti-GAD_{65} encephalitis. Six of the rhuMAb reconstructed from cePc, namely GKD3, GKD4, GKD5, SSM5, JMB2 and JMB3, showed a clear reactivity to their presumed cognate target antigens *in vitro*.

Our findings provide evidence that clonally expanded intrathecal plasma cells/blasts contribute to the production of antineuronal autoantibodies in AIE patients. By reconstructing functional autoantibodies from CSF cePc in the form of rhuMAb, we demonstrate the presence of a CNS-specific antigen driven humoral immune response in the CSF compartment of AIE patients. Having patient derived antineuronal autoantibodies in recombinant monoclonal form may be an appropriate tool to analyse their precise epitope specificity and functional properties, which may help to understand the exact mechanisms of their role in disease pathogenesis. Some of the patient derived antineuronal rhuMAb could also be used to study their therapeutic usefulness in other neurological diseases, in which it may be beneficial e.g. to block NMDA receptor mediated excitotoxicity.

Als „Autoimmun-Enzephalitis“ (AIE) wird eine Gruppe von Syndromen genannt, die durch Autoantikörper gegen synaptische oder neuronale Zelloberflächen-Proteine gekennzeichnet sind. Frühere Studien, die mithilfe von Serum und Liquor (engl. cerebrospinal fluid, CSF) von AIE Patienten durchgeführt wurden, beschrieben antineuronale Autoantikörper, die spezifisch gegen den AMPA-Rezeptor, NMDA-Rezeptor, leucine-rich glioma inactivated protein 1 (LGI1), contactin-associated protein-like 2 (CASPR2) oder Glutamat Decarboxylase (GAD_{65}) gerichtet sind. Um Ursprung und Funktion der intrathekalen Autoantikörper bei AIE Patienten näher zu charakterisieren, war es Ziel dieser Arbeit, das Immunrepertoire intrathekaler $CD138^{+}$ Plasmazellen zu untersuchen und einige der antineuronalen Autoantikörper in Form von rekombinanten humanen monoklonalen Antikörpern (rhuMAb) nachzubilden.

Zu diesem Zweck analysierten wir 584 einzelne, FACS sortierte Plasmazellen aus dem Liquor von fünf AIE Patienten mit Hilfe der Einzelzell-RT-PCR und konnten von 508 Zellen die Immunglobulin Schwerkettensequenz ermitteln. Durch Analyse der CDR3-Sequenzen wiesen wir in allen untersuchten Liquor-Zellproben klonal expandierte Plasmazellen (cePc) nach und identifizierten insgesamt 57 unabhängige Plasmazell-Klone. Zudem untersuchten wir die relative Häufigkeit der Immunglobulin-Gen-Familien: Ein Patient mit gesicherter anti-LGI1-Autoimmun-Enzephalitis (Patient GKD) zeigte eine klare Überrepräsentation der V_H4 Familie. Die V_H1 Familie war dahingegen bei einem Patienten mit anti-NMDA-Rezeptor Enzephalitis (Patient SSM) unterrepräsentiert. Zwei Patienten mit CASPR1 Autoantikörpern (Patienten KKM & BRM) hatten ähnliche Verteilungsmuster der VH-Genfamilien in folgender Reihenfolge der Häufigkeiten: $V_H3>V_H1>V_H4>V_H5$. Nur bei einem Patienten mit anti-CASPR2 Autoantikörpern konnten auch Amplikons der V_H7 Familie zugeordnet werden. Die V_H1 Sequenz-Familie war hauptsächlich in einem Patienten mit GAD_{65} (JMB) Autoantikörpern präsent.

Um herauszufinden, ob cePc die tatsächlichen Produzenten der intrathekalen Autoantikörper Antwort sind, klonierten und exprimierten wir die zueinander gehörenden Immunglobulin Schwer- und Leichtkettengene von 16 expandierten Plasmazellklonen und von einer nichtexpandierten Plasmazelle von drei der fünf AIE Patienten und stellten dadurch exakte Kopien der intrathekalen Autoantikörper her. Jeweils sieben rhuMAb (SSM1-7 bzw. GKD1-7) wurden von einem Patienten mit anti-NMDA-Rezeptor bzw. anti-LGI1-Enzephalitis generiert. Drei weitere Antikörper (JMB1-3) wurden aus den cePc Klonen eines Patienten mit anti-GAD_{65} Enzephalitis hergestellt. Sechs der rekonstruierten 17 Antikörper (GKD3, GKD4, GKD5, SSM5, JMB2 und JMB3) zeigten eine klare Reaktivität gegen die vermuteten Ziel-Antigene *in vitro*.

Unsere Untersuchungen zeigen, dass klonal expandierte intrathekale Plasmazellen zur Produktion von antineuronalen Autoantikörpern beitragen. Durch die Rekonstruktion von funktionalen, humanen, monoklonalen Autoantikörpern aus den CSF cePc in Form von rhuMAb wiesen wir zudem eine ZNS-spezifische humorale Immunantwort im

Liquorkompartiment von AIE Patienten nach. Antineuronale Autoantikörper, die ausgehend vom Patientenmaterial in rekombinanter, monoklonaler Form rekonstituiert werden, stellen sehr gute Werkzeuge für die funktionelle Charakterisierung, Epitopentschlüsselung und detaillierte Untersuchung der Antikörper-Beteiligung an der AIE Pathogenese *in vitro* und *in vivo* dar. Einige dieser Antikörper könnten zudem von therapeutischem Nutzen sein bei neurologischen Erkrankungen, die z.B. von einer Blockade NMDA-Rezeptor mediierter Exzitotoxizität profitieren.

INTRODUCTION

The immune system defends the body against invading foreign objects or internal invaders such as tumors, by complex interactions and activities of a large number of diverse immune cells. The innate immune response is the first line of defense and occurs soon after pathogen exposure. It is carried out by phagocytes such as neutrophils, macrophages, cytotoxic natural killer cells, and granulocytes. The subsequent adaptive immune response includes antigen-specific defense mechanisms and may take days to weeks to build up. Antigen-dependent activation of various cell types of adaptive immune system such as T cells, B cells, macrophages, dendritic cells and other antigen-presenting cells (APCs) play critical roles in host defense mechanism. The B cells having been exposed to antigen become plasma cells and produce large amounts of antibodies. Other functions of B cells are antigen-presentation, and to develop into memory B cells after activation by antigen interaction.[1]

Immunoglobulins (Ig) are glycoproteins found in body fluids such as blood, CSF, tissue fluids, as well as in many secretions such as tears, saliva, etc. The main function of an antibody is to identify and neutralize foreign objects like bacteria, viruses and others, via binding to a very specific and unique antigen target. Antibodies binding to their specific antigens cause agglutination and precipitation of antibody-antigen products, making them easier targets for phagocytosis by macrophages and other cells, block viral receptors, and stimulate other immune responses, such as complement system.

The structure of an antibody molecule is roughly Y-shaped, the molecular weight is around 150 kDa; it consists of two identical heavy chains, each approximately 50 kDa, and two identical light chains, each approximately 25 kDa, connected by disulfide bonds (**Fig. 1,** Pg.5). Each light and heavy chain of an antibody contains two major regions, a variable and a constant region. The variable region of each heavy and light chain ends at the N-terminus, highly diverse in amino acid sequences, and determine the unique antigen specificity of the antibody. There are three loops in the variable regions of each chain, known as hypervariable regions or complementarity-determining regions (CDRs), which fold and come together to form the antigen-binding sites at the amino-terminal end of the antibody. About 85% of the variable regions are intervening sequences between the CDRs known as framework residues (FR), which define the positioning of the CDRs and have restricted variability and show little difference in amino acid sequence between chains. When the

variable regions of light and heavy chains come together, the CDRs of the both chains form a cleft that serves as the antigen-binding site of an antibody.[2] The antigen-binding sites or complementarity-determining regions are also called idiotypes, which makes any antibody unique from others of the same type.

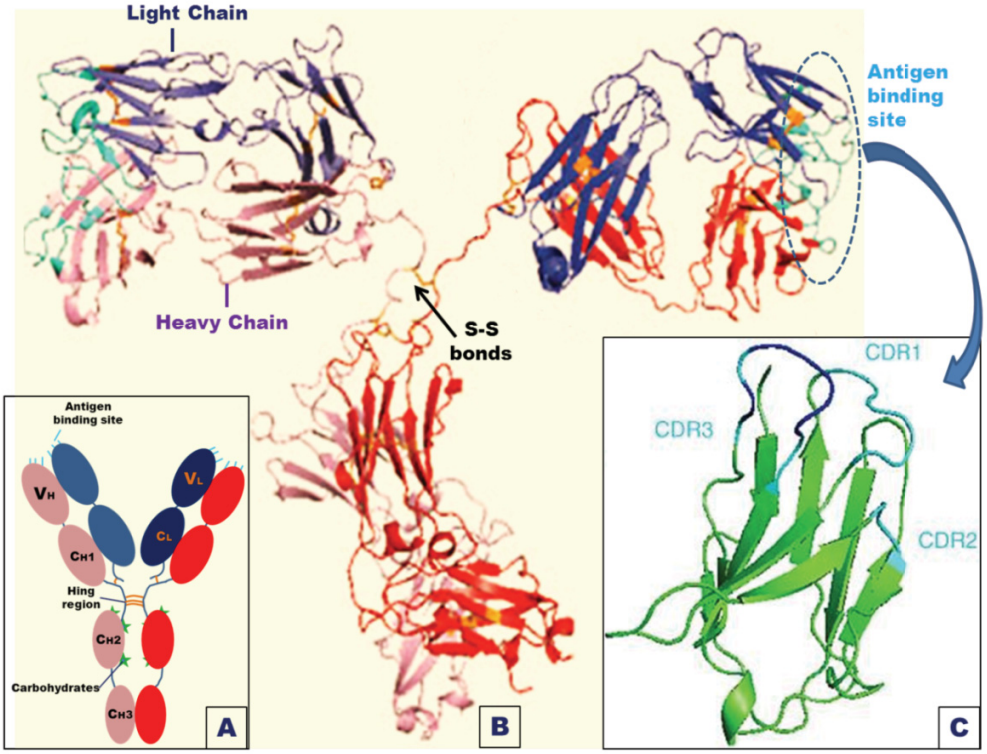

Figure: 1. Schematic representation of IgG structures shown in drawing form (A), and in ribbon form (B). The heavy chains are shown in red and pink, light chains in blue and light blue. The inter- and intra-chain disulfide bonds are in orange, the complementarity determining regions (CDRs) in cyan. The structure of the variable region has a β-sheet framework with three loops called the complementarity determining regions (CDR1, CDR2 and CDR3) in each heavy and light chain (**C**). These CDRs are highly variable and mainly involved in binding their respective antigen through van der Waals force, hydrogen and ionic bonds. Especially the CDR3, which is the loop with the highest variable amino acid composition and length, is primarily involved in the binding to the antigen. Figure adapted with modifications.[3]

Constant regions of the light and heavy chains end at the C-terminus and do not vary in amino acid sequences within a given class. The constant regions are also called isotype, which determines the class and subclass of the antibodies. In human, there are five different heavy chain isotype (constant region) classes, namely IgM, IgD, IgE, IgG and IgA; in addition, there are four subclasses of IgG, namely IgG1, IgG2, IgG3 and IgG4, and two subclasses of IgA, namely IgA1 and IgA2, giving a total of nine different classes and subclasses for immunoglobulin heavy chain (**Table 1**, Pg.7&8). There are two different light chain isotype classes, namely kappa (Igκ) and lambda (Igλ); although Igκ chain has no subclass, there are four subclasses of Igλ chain, namely Igλ1, Igλ2, Igλ3 and Igλ4. Either Igκ or Igλ chain can be found associated with any class or subclass of heavy chains, but not both, in any given antibody. In the light chains, constant regions are about the same size as the variable regions, whereas in the heavy chains, constant regions are three to four times larger than the variable regions depending on the heavy chain isotype (**Table 1**, Pg.7&8)

The humoral adaptive immune system is able to produce an enormous diversity of antibodies to fight specific pathogens by V(D)J recombination mechanism. There are scattered gene segments known as variable (V), diversity (D) and joining (J) on chromosome 14, which encodes the heavy chain variable regions of antibodies and also B and T cells receptors. The random V(D)J gene segments recombination in the bone marrow for B cells and in the thymus for T cells, generating a large number of variable regions to cope with different kind of antigens. In case of B cells, two additional mechanisms, namely somatic hypermutations (SHMs) and class switch recombination (CSR), triggered after antigen recognition, further optimize the antibody response (**Fig. 2**, Pg.10). Accumulation of somatic hypermutations within the V gene segment of antibody increases its affinity for antigen. Class switch recombination (CSR) mechanism allows a previously rearranged heavy chain variable domain to be expressed in association with a different constant region, leading to the production of different isotypes such as IgG, IgA or IgE, which mediate antigen elimination by different routes without changing antibody specificity. The kappa (κ) and lambda (λ) light chains gene loci on chromosome 2 and 22 respectively, rearrange in a very similar way, except the light chains lack a D segment.

IgG 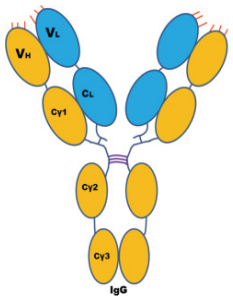	Most abundant serum Ig (75%). Four subclasses, namely IgG1 (66%), IgG2 (23%), IgG3 (7%) and IgG4 (4%), all could fix complement either via classical or alternate pathway. Around 150 kDa monomeric antibody, contains two gamma (γ) heavy chains, each having 3 constant domains (Cγ1-Cγ3), pairs with either kappa or lambda light chain. Produced late in immune responses and can be transferred across the placenta into the fetal circulation. Opsonizing activity via Fc receptors present on macrophages and polymorphonuclear cell family (PMNs). IgG titers and oligoclonal bands are used as diagnostic tools. IgG antibodies are extracted from donated blood plasma and used as a therapeutic known as intravenous immunoglobulin (IVIG). This is used to treat immune deficiencies, autoimmune disorders and infections.
IgA 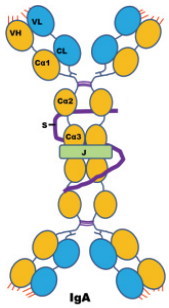	Most abundant secretory Ig (10-15%) in exocrine secretions such as tears, saliva, bile, mucus of the gut, respiratory tract, ears, vagina, milk, etc. Around 385 kDa dimeric antibody, monomer contains two alpha (α) heavy chains, each having 3 constant domains (Cα1-Cα3), pairs with either kappa or lambda light chain; found in two subclasses, namely IgA1, IgA2, all can exist mostly in a dimeric form with some monomeric and trimeric forms, linked by J-piece (for joining) and an S-piece (secretory). Provide protection against microbes that multiply in body secretions. IgA is a poor activator of the complement system, and weak in inducing opsonises.
IgM 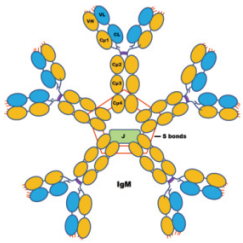	Second most abundant serum Ig (5-10%). First antibody to appear in blood and lymph fluid in response to initial exposure to an infection and most efficient Ig at complement fixation. Around 970 kDa pentameric antibody, monomer contains two mu (μ) heavy chains, each having 4 constant domains (Cμ1-Cμ4), pairs with either kappa or lambda light chain; exist mostly in a pentameric form with some hexamer, linked together with disulfide bonds and a J-piece (joining). Monomeric forms serve as membrane receptors of B-cells. IgM antibodies are mainly responsible for the clumping of red blood cells if the recipient of a blood transfusion receives blood that is not compatible with their blood type.

Table 1. Characteristics of different kinds of immunoglobulin molecules.

Ig**D** 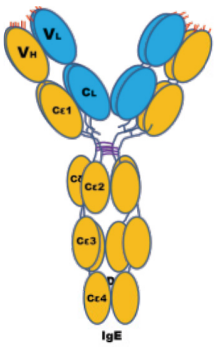 	Found in low concentration about (1%) of total serum Ig. Around 150 kDa monomeric antibody contains two delta (δ) heavy chains, each having 3 constant domains (Cδ1-Cδ3), pairs with either kappa or lambda light chain. Mainly found on the B-cells as membrane receptor. Signals the B cells to be activated in response to antigen encounter. Secreted form of IgD in the blood plasma binds to basophils, mast cells and activates these cells to produce antimicrobial factors to participate in respiratory immune defense.
Ig**E**	Extremely low levels in serum (0.05%). Around 190 kDa monomeric antibody, contains two epsilon (ε) heavy chains, each having 4 constant domains (Cε1-Cε4), pairs with either kappa or lambda light chain. Reaginic antibody, responsible for allergic reactions following binding to surface of tissue mast cells. Capable of triggering the most powerful inflammation reactions. Mostly found in the lungs, skin, and mucous membranes. Its main function is immunity against foreign substances such as parasitic worm, protozoa, pollen, fungus spores, etc. It is involved in allergic reactions to milk, some medicines, and some poisons.
Table 1. continued.	

Usually, any V(D)J recombinations in B cells producing self-reactive autoantibodies are eliminated by the clonal deletion mechanism. However, due to some not yet well understood reasons, autoantibodies have been detected targeting self-antigens in different kind of autoimmune diseases, such as autoimmune limbic encephalitis,[5] myasthenia gravis,[6] neuromyotonia,[7] stiff person syndrome,[8] Neuromyelitis optica,[9] and several more. These autoantibodies attack the body's own healthy cells, tissues, and/or organs, causing inflammation and damage.[10] It should be noted that autoantibodies may also play a nonpathological role; for instance they may help the body to destroy cancers and to eliminate waste products. The role of autoantibodies in normal immune function is also a subject of scientific research.

Autoantibodies in AIE

The autoimmune encephalitis (AIE) syndromes are a group of conditions that are associated with autoantibodies against neuronal proteins, which are likely to be involved in disease pathogenesis. A pathogenic role of these antibodies is supported by the response of clinical symptoms to immunotherapy, immunoglobulin (Ig) deposits in patients' CNS and transfer experiments. In a part of the cases, the autoantibodies are associated with the presence of a remote tumor (paraneoplastic), but more often these diseases are non-paraneoplastic and the trigger is unclear. The autoimmune limbic encephalitis syndromes typically produces subacute memory impairment, confusion and seizures. Other clinical and paraclinical findings vary depending on the underlying cause.

Based on the targets of the autoantibodies, AIE can be classified into two types:

- **Antibodies specific for intracellular antigens**
- **Antibodies specific for neuronal cell surface antigens**

Generally, antibodies specific for intracellular antigens are associated with underlying malignancies whereas those specific for membrane antigens are not necessarily associated with the presence of a tumor. However, some membrane autoantibodies may be associated with tumors as well (**Fig. 3**, Pg.12).

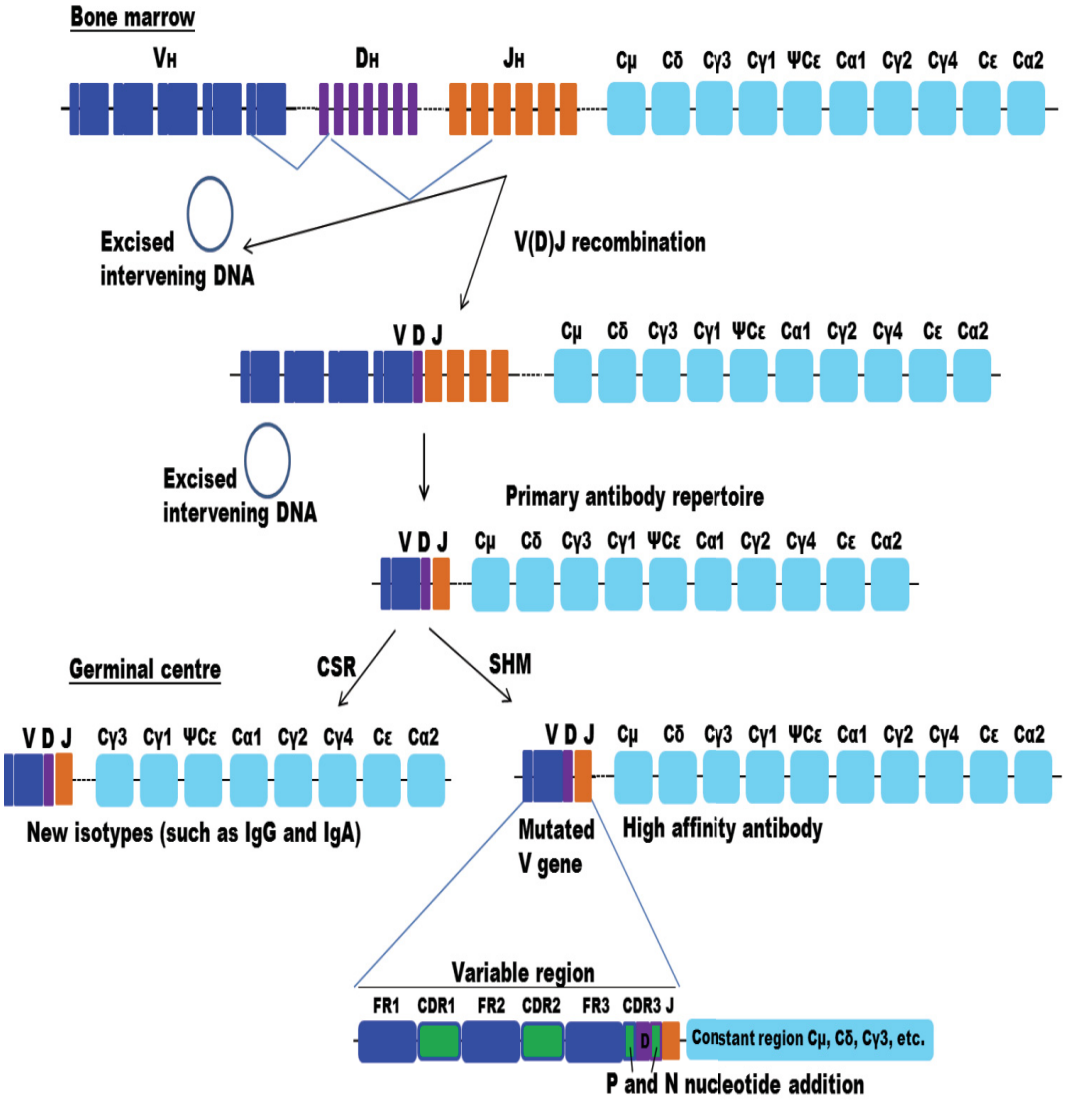

Figure: 2. Organization of the human immunoglobulin IgH locus and its somatic modifications. In its germline configuration, the variable domain of IgH is composed of clusters of gene segments encoding variable (**V, blue boxes**), diversity (**D, purple boxes**) and joining (**J, orange boxes**) exons. The V(D)J recombination leads to the formation of a VDJ-rearranged productive gene unit that is formed by the physical link between these three exons. The intervening DNA is excised as circles. During class-switch recombination (**CSR**), a new rearrangement process leads to the association of the VDJ unit to another constant (**C**) region exon. The intervening DNA is also excluded from the chromosome as a circle. High-affinity antibodies are obtained through the accumulation of somatic hypermutations (**SHMs**) in the V genes. Figure adapted with modifications.[4]

- **Antibodies specific for intracellular antigens**

These autoantibodies are directed against intracellular targets and often referred to as 'onconeural antibodies' as they are almost exclusively, associated with a paraneoplastic limbic encephalitis. Common examples include those directed against Hu (ANNA-1), Ma2, CV2/CRMP5, Amphiphysin and Glutamic Acid Decarboxylase (GAD). These are usually associated with cytotoxic T cell mechanisms. Clinical syndromes are diverse, neuronal damage seems to be irreversible and although some improvement may occur after identification and removal of the primary tumor, the prognosis in general is poor.[11] One exception appears to exist in patients with anti-GAD autoantibodies: these patients may have autoimmune limbic encephalitis, epilepsy or other neurological syndromes, while tumors are uncommon. Recovery is possible although patients are often less responsive to immunotherapies.[12]

Anti-GAD encephalitis

Anti-GAD autoantibodies target an intracellular enzyme called glutamic acid decarboxylase (GAD). In mammalians, GAD exists in two isoforms GAD_{67} and GAD_{65} with molecular weights of 67 and 65 kDa encoded by two different genes GAD1 and GAD2 respectively.[13] GAD1 and GAD2 are expressed in the brain where GABA is used as a neurotransmitter; GAD2 is also expressed in the pancreas. The GAD_{65} enzyme is usually found associated with the membrane of synaptic vesicles at the nerve terminal and probably plays a specific role in the control of the synaptic release of GABA.[129] These enzymes are responsible for converting glutamic acid to GABA, a neurotransmitter found in high concentrations in the cerebellum. It is believed that the lack of GABA results in cerebellar ataxia.[14] The anti-GAD autoantibodies have also been associated with a disease characterized by stiffness of the muscles, called "stiff person syndrome",[8] diabetes mellitus type 1, thyroid disease and rheumatoid arthritis.[15]

Anti-GAD autoantibodies have also been recently associated with autoimmune limbic encephalitis, although this is not usually paraneoplastic. It is mostly associated with temporal lobe epilepsy, memory loss, behavioral abnormalities, and psychosis.[16,17,18] Corticosteroid therapy, plasma exchange and infusion of immunoglobulin intravenously (IVIG) are the most common treatments for anti-GAD AIE.[8]

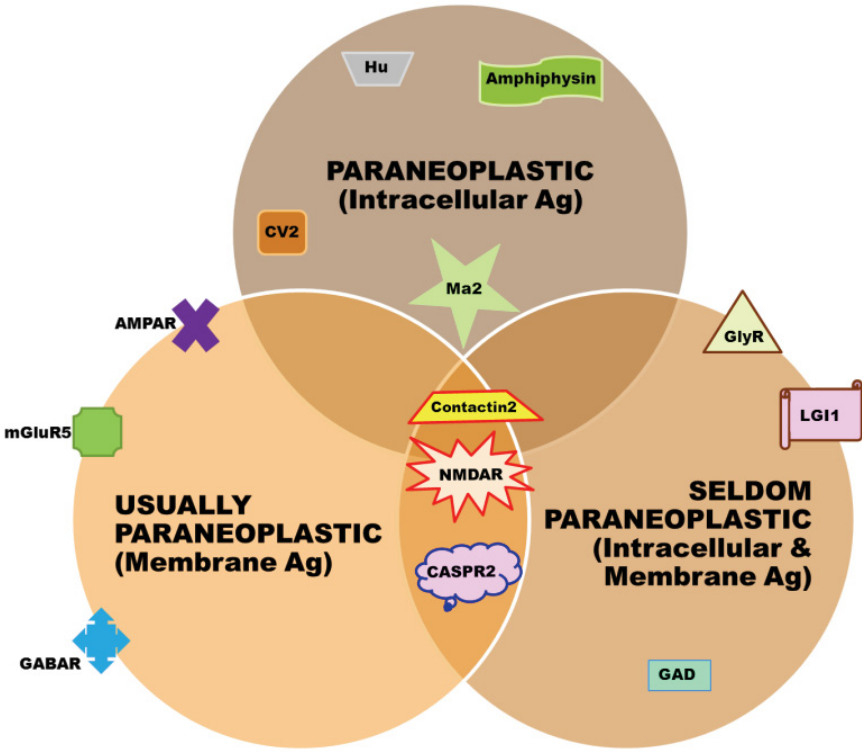

Figure: 3. Venn diagram depicting clinical findings that are shared among different types of autoimmune encephalitis (AIE).
Autoantibodies targeting intracellular or membrane antigens (Ag) associated with non-paraneoplastic and paraneoplastic syndromes. Although paraneoplastic syndromes usually associated with intracellular antibodies such as Anti-Hu, Anti-Ma2 etc., it may also be associated with membrane antibodies such as anti-AMPAR,[19] anti-GABAR.[20] The clinical features of anti-NMDAR autoantibody overlap among different types of AIE. Therefore, even in the presence of membrane antibodies, a search for an underlying malignancy should be considered. GlyR: Glycine receptor; LGI1: Leucine-rich glioma inactivated 1 protein; GAD: glutamic acid decarboxylase.

- **Antibodies specific for neuronal cell surface antigens**

These antibodies are usually directed against membrane antigens on pre- or post-synaptic sites of the neurons and often associated with non-paraneoplastic limbic encephalitis and have a better prognosis. The cognate targets of some of these antibodies have been identified, e.g voltage-gated potassium channel (VGKC)-complex, NMDA receptor, AMPA

receptor, Glycine receptor, GABA receptor and mGluR5. The common symptoms are memory deficits, headache, irritability, sleep disturbance, delusions, hallucinations, agitation, seizures and psychosis.[21] Examination of cerebrospinal fluid (CSF) of the patients shows elevated levels of lymphocytes, CSF protein, IgG index and oligoclonal bands. Patients with antibodies to voltage-gated potassium channels (VGKC) may have a completely normal CSF examination[22,23,24]. Patients often respond to immunotherapies such as intravenous immunoglobulins, plasma exchange, corticosteroids, cyclophosphamide and/or rituximab. If an associated tumor is found, then recovery is not possible until the tumor is removed.[21]

Different kind of neuronal cell surface antigens associated AIE are summarized below.

Anti-VGKC encephalitis

The voltage-gated potassium channel (VGKC) is composed of alpha (α) and beta (β) subunits of Kv1 channels and is tightly associated with other proteins including contactin-associated protein-like 2 (CASPR2); contactin-2 (also known as TAG-1) and ADAM 22/23 in mammalian neuronal membranes.[25,26,27] Leucine-rich glioma inactivated 1 protein (LGI1) is a neuronally secreted protein that associates with the VGKC complex via binding to ADAM22 and ADAM23 (**Fig. 4**, Pg.14).[28,29] ADAM22 also associates separately with AMPA receptors. LGI1 can also concurrently associate with two ADAM22 proteins bound to a VGKC complex and AMPA receptor.[30,31]

Anti-VGKC autoantibodies are reported in patients with peripheral nerve symptoms like Neuromyotonia, characterized by cramps and fasciculations;[32,7] Morvan's syndrome, characterized by neuromyotonia with autonomic, cognitive and sleep disturbances;[33,34] Faciobrachial Dystonic Seizure, characterized by brief but frequent dystonic epileptic events in arm and the ipsilateral face;[35] and Limbic encephalitis, these patients usually present with seizures, confusion and subacute memory loss.[23,36] In all these conditions, the VGKC-complex antibody levels fall in response to immunotherapy, which commonly involves intravenous immunoglobulins or plasma exchange. This is usually accompanied by a clinical improvement.

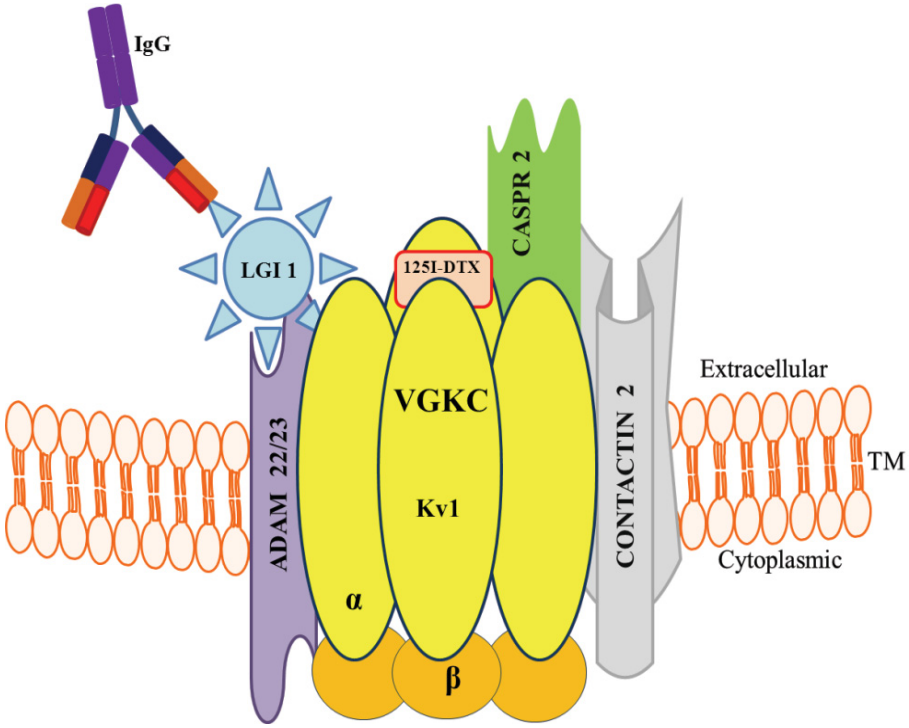

Figure: 4. Schematic representation of the voltage-gated potassium channel (VGKC) and associated proteins.
The VGKC is composed of alpha (α) and beta (β) subunits of Kv1 channels and is complex with other proteins including CASPR2, contactin-2 and ADAM 22/23 in mammalian brain membranes. LGI1 is a neuronally secreted protein that associates with VGKC complex via binding to ADAM22 and ADAM23. Anti-LGI1 autoantibodies specifically inhibit the ligand-receptor interaction between LGI1 and ADAM22/23 by targeting the EPTP repeat domain of LGI1. VGKC complex proteins are co-immunoprecipitated in radioimmunoprecipitation assays using ^{125}I-α-dendrotoxin (^{125}I-DTX) detergent. Autoantibodies against LGI1, CASPR2 and CONTACTIN 2 are found in AIE and other autoimmune diseases. Figure adapted with modification.[7,37]

It was recently reported that anti-VGKC complex associated autoantibodies detected by using an ^{125}I-α-dendrotoxin-labelled radioimmunoprecipitation assay, generally do not bind to VGKC channel proteins per se, but they bind instead to synaptic and axonal neuronal proteins that co-precipitate with detergent-solubilized VGKCs.[38,39] These 'VGKC-complex' antigenic targets include:

- Leucine-rich glioma inactivated 1 protein (LGI1)
- Contactin-associated protein-like 2 (CASPR2)
- Contactin-2

Anti-LGI1 autoantibodies specifically inhibit the ligand-receptor interaction between LGI1 and ADAM22/23 by targeting the EPTP repeat domain of LGI1 (**Fig. 4**, Pg.14) and reversibly reduce the synaptic AMPA receptor clusters in rat hippocampal neurons[31]. They are most commonly seen in patients with limbic encephalitis or epilepsy with neuropsychiatric features, amnesia, confusion, serum hyponatremia, seizure, and usually without tumors.[38,39] In contrast, anti-CASPR2 autoantibodies are found in patients with limbic encephalitis, Morvan's syndrome or Neuromyotonia, often with tumor, including thymoma.[40,41] Anti-Contactin-2/Tag-1 autoantibodies are least commonly detected and are often associated with Morvan's syndrome.[42,39]

As LGI1 is almost exclusively expressed in central nervous system neurons and CASPR2 in both the central and peripheral nervous systems, the autoantibodies are considered to be mediators of the diseases. While careful correlations between antibody levels and clinical outcomes in individual patients, in combination with passive transfer experiments in animals, are required to formally assess VGKC-complex autoantibody pathogenicity, it has been proven that LGI1-antibodies can generate seizure like activity in hippocampal slice cultures.[43] Interestingly, further evidence for the disease relevance of these proteins comes from known genetic variations. Human LGI1-mutations produce a lateral temporal lobe epilepsy syndrome[44] and mice lacking LGI1 show a variety of motor semiologies.[45] Humans with CASPR2 mutations present autism, seizures, and peripheral neuropathy.[46]

Anti-NMDA receptor encephalitis

The N-methyl-D-aspartate receptor (NMDA receptor) is an ionotropic glutamate receptor regulating synaptic plasticity and memory function.[47] The NMDA receptors are heterotetrameric proteins containing two obligatory NR1 (GluN1) subunits and two regionally localized NR2 (GluN2) subunits with an extracellular N-terminus, intracellular C-terminus and a reentrant transmembrane domain (**Fig. 5**, Pg.17).[48,49] The NR1 subunit is an

essential component of all NMDA receptor complexes and has eight variants produced by alternative splicing of GRIN1 namely NR1-1a, NR1-1b; NR1-2a, NR1-2b; NR1-3a, NR1-3b; NR1-4a and NR1-4b.[128] NR1-1a is the most abundantly expressed form. There are four NR2 subunits (NR2A-D) that are products of separate genes. Multiple receptor isoforms with distinct brain distributions and functional properties arise by selective splicing of the NR1 transcripts and differential expression of the NR2 subunits. Thus, NMDA receptors in different parts of the brain, or at different stages in development, may not act in the same way. A related gene family of NR3 A and B subunits has an inhibitory effect on receptor activity. Calcium flux through NMDA receptor is critical in synaptic plasticity and an important mechanism for learning and memory. The NMDA receptor is both ligand-gated and voltage-dependent and requires co-activation by two ligands: glutamate and either glycine or D-serine,[50] and can be blocked by extracellular Mg^{2+} & Zn^{2+} ions.[51] Hyperactivity of NMDA receptors causing excitotoxicity is a proposed underlying mechanism for epilepsy, dementia, and stroke, whereas low activity produces symptoms of schizophrenia.[52,53,54]

Autoantibodies against the extracellular N-terminus of NR1 subunit of NMDA receptor were first reported by Josep Dalmau, in CSF and serum of patients, usually females, with paraneoplastic limbic encephalitis presented with combinations of prominent psychiatric symptoms, amnesia, seizures, frequent dyskinesias, autonomic dysfunction, and decreased level of consciousness.[7,55] Although primarily a paraneoplastic syndrome of young women with ovarian teratomas, an increasing number of cases have been reported in both men and women, in retrospective cohorts of adults or children ranging in age from 11 months to 76 years, with and without tumors.[55,56,57,58,59]

It has been proposed that an immune-mediated mechanism underlies this syndrome; antibodies formed against neoplastic cells cross-react with native NMDA-receptors leading to rapid internalization of surface NMDAR clusters in both excitatory and inhibitory hippocampal neurons (**Fig. 5**, Pg.17).[58,60] In other studies, it is suggested that Herpes simplex virus 1 infection can trigger anti-NMDAR receptor encephalitis, usually between 4 and 6 weeks after herpes simplex encephalitis.[61]

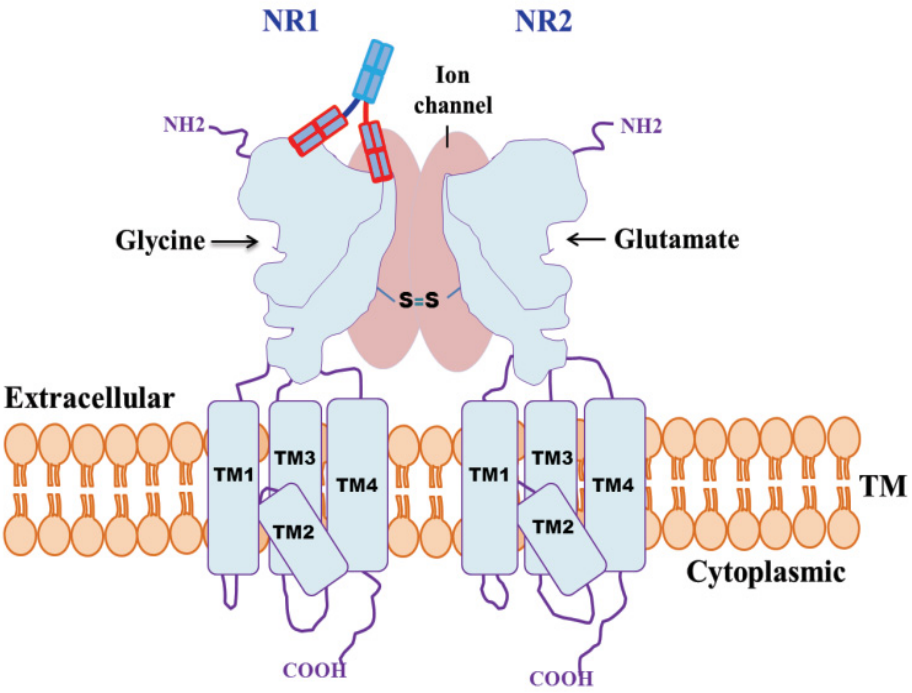

Figure: 5. Schematic representation of a basic NMDA receptor.
Receptor contain extracellular N-terminus regions which involved in ligand binding, transmembrane motif TM1-4, and cytoplasmic C-terminus region which interact with intracellular molecules for postsynaptic signalling. Binding of magnesium ion blocks the ion channel in a voltage-dependent manner, whereas binding of glutamate and glycine removes this block and open the channel for calcium to inter. Binding of autoantibodies to the extracellular N-terminus of NR1 subunit leads to rapid internalization of surface NMDAR clusters in both excitatory and inhibitory hippocampal neurons.[58,60] Figure adapted with modifications.[49,62,63]

NR1 and NR2 heteromers predominate within the hippocampus, with less intense reactivity described in the forebrain, basal ganglia, spinal cord and cerebellum.[58,64] Thus, autoantibodies may preferentially affect areas responsible for memory, personality, movement and autonomic control, accounting for the unique confluence of personality changes, impairments in cognition, motor derangements and disturbances in respiratory drive that define the syndrome. Antibody titers are higher in patients with confirmed

malignancies and highest in those with the most severe symptoms. The autoantibodies demonstrate in vitro evidence of pathogenicity and the patients respond well to immunotherapies such as steroids, intravenous immunoglobulin, plasmapheresis, rituximab, cyclophosphamide, and tumor removal.[65]

Anti-AMPA receptor encephalitis

The α-amino-3-hydroxy-5-methyl-4-isoxazolepropionic acid receptor (AMPA receptor) is an ionotropic transmembrane receptor for glutamate that mediates synaptic transmission in the central nervous system (CNS). Its name is derived from the ability to be activated by the artificial glutamate analog AMPA. The AMPA receptors are composed of 4 subunits GluR1-4 also known as GluR- A-D, which are widely, but differentially, distributed throughout the CNS.[66] The types of subunits forming these receptors determine their biophysical properties and pharmacological sensitivity. The AMPA receptors containing the GluR2 subunit are widely distributed throughout the CNS and play a key role in synaptic transmission and plasticity, for example long term potentiation or LTP.[67,68] Two alternative splice variants of GluR1 to GluR4 subunits designated as 'flip' and 'flop' have been shown to differ in their expression throughout the brain and during development and to impart different pharmacological properties, (**Fig. 6**, Pg.19).[69,70] AMPA receptors play a key role in the generation and spread of epileptic seizures.[71]

Anti-AMPA receptor autoantibodies directed against GluR1, GluR2 and peptide B of GluR3 (GluR3B) subunits of the AMPA receptors are reported in serum and CSF of limbic encephalitis patients. Patients present with personality changes resembling psychosis, followed by seizures; variation in consciousness and autonomic labiality, sometimes associated with an underlying neoplasm usually breast, thymus, or lung that expresses AMPA receptors.[19,72,73] The most commonly affected brain areas are hippocampus, cerebral cortex, basal ganglia, and cerebellum as they expresses high level of GluR1&2 suggesting that the clinical presentation could also extend beyond the clinical profile of limbic encephalitis.[74,75,19]

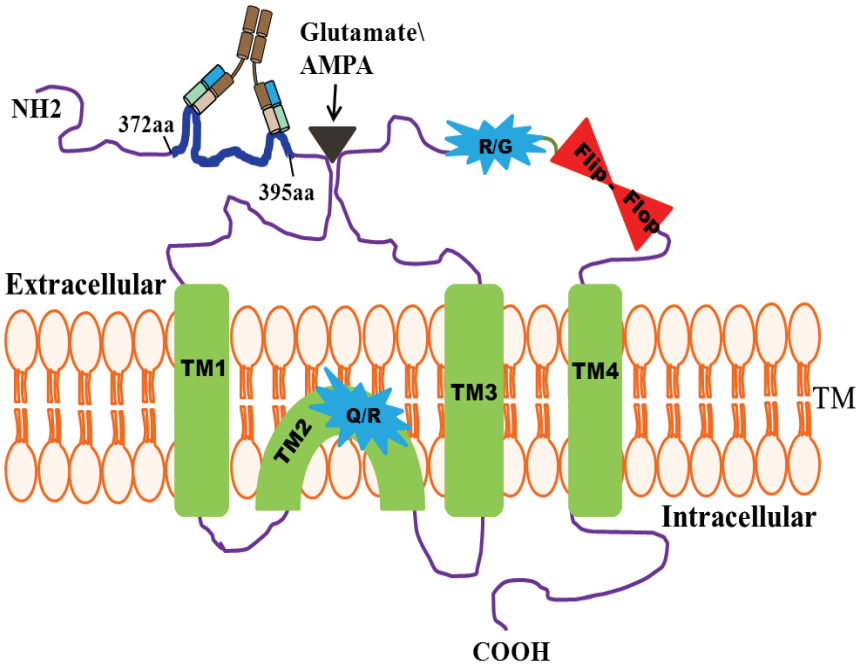

Figure: 6. Schematic representation of a basic AMPA receptor subunit.
Showing extracellular N-terminus regions which involved in ligand binding, transmembrane motif TM1-4, and cytoplasmic C-terminus region. The flip-flop module between TM3 and TM4 is generated by alternative splicing. The Q/R site and R/G site indicate the positions where RNA editing occurs.[130] Autoantibody directed against amino acids 372—395 of GluR3B subunit (blue line) leads to neurological and psychiatric abnormalities. Anti GluR1/2 autoantibodies can alter the synaptic localization and number of AMPA receptors in neuronal culture.[76, 73, 19]

It has been shown that anti-AMPA receptor autoantibodies directed specifically against amino acids 372—395 of GluR3B subunit, can by themselves activate GluR3-containing glutamate/AMPA receptors, evoke ion currents via the receptor's ion channel, kill neurons and damage the brain (**Fig. 6**).[73,76] The anti-GluR3B autoantibodies also associate with neurological, psychiatric and behavioral abnormalities in epilepsy patients[73] and also induce abnormal behavior in mice.[76] Application of anti-GluR1/2 subunit autoantibodies to neuronal cultures significantly alter the synaptic localization and number of AMPA receptors.[19]

Anti-Glycine receptor encephalitis

The glycine receptors (GlyRs) are widely distributed inhibitory receptors in the central nervous system (CNS), mainly in the spinal cord, brainstem and caudal brain, and control a variety of motor and sensory functions, including vision and audition.[77,78] The structure of GlyRs is pentameric, transmembrane, consists of five homomeric and/or heteromeric subunits arranged around a central pore to form chloride ion channels, which mediates most of the fast inhibitory synaptic transmission in the brain (**Fig. 7**, Pg.21). Four α-subunit isoforms (α_{1-4}) and a single β-subunit isoform of GlyRs have been identified in the vertebrate.[79, 80, 81] The β-subunit determines the ligand binding properties of synaptic glycine receptors. The adult form of the GlyR is the heteromeric $\alpha_1\beta$ receptor, which seems to have a stoichiometry of $2\alpha_1$:3β.[82, 83] The α-subunits are also able to form functional homo-pentameric receptors and are essential for studies on channel pharmacokinetics and pharmacodynamics.[84] Binding of glycine leads to the opening of the GlyR's integral anion channel, and the resulting influx of Cl^- ions hyperpolarizes the postsynaptic cell, thereby inhibiting neuronal firing. Disruption of GlyRs surface expression, or reduced ability of expressed GlyRs to conduct chloride ions, results in a rare neurological disorder, hyperekplexia. This disorder is characterized by an exaggerated response to unexpected stimuli which is followed by a temporary but complete muscular rigidity often resulting in an unprotected fall.[85]

Anti-Glycine receptor autoantibodies (anti-GlyR-ab) were first described in patients with spinal and brainstem disorders. The majority of the patients with anti-GlyR-ab have progressive encephalomyelitis with rigidity and myoclonus (PERM).[86] The anti-GlyR-abs activate complement proteins by binding to the α1 subunits of GlyR (GLRA1) expressed on the surface of transfected HEK-293 cells at room temperature, and cause internalization and lysosomal degradation of the glycine receptors at 37°C and also immunoprecipitated GlyRα1.[86, 87] Since then, further patients with anti-GlyR-ab have been described with combinations of stiffness, rigidity, excessive stimulus-evoked startle, brainstem and autonomic signs.[88, 89, 90]

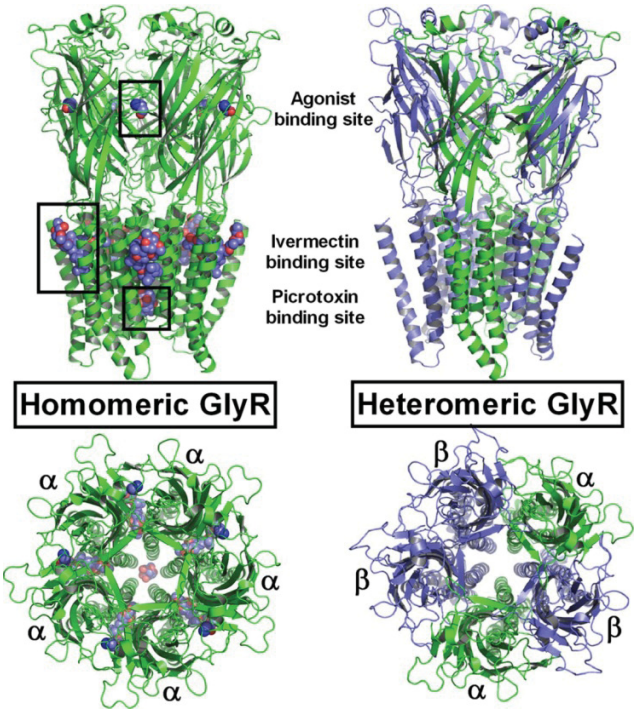

Figure: 7. Schematic representation of homomeric α1 and heteromeric α1β-glycine receptors (GlyRs) in ribbon forms, using glutamate-gated channel (GluCl) as a template.
The structure of GlyRs are pentameric, transmembrane, consists of either five homomeric $\alpha 1_5$ subunits (**left**) or heteromeric $\alpha 1_2\beta_3$ subunits (**right**) arranged around a central pore to form chloride ion channels, which mediates most of the fast inhibitory synaptic transmission in the brain. Figure adapted with permission.[84]

The symptoms of PERM are similar to stiff person syndrome (usually an anti-GAD-ab syndrome), with rigidity, stimulus-sensitive spasms, myoclonus, hyperekplexia and autonomic disturbance, but with additional brainstem or other neurological defects. Anti-GlyR-ab has also been found in retrospective cohorts of adults or children, with or without GAD autoantibodies.[91, 92, 93] Serum autoantibodies to both glycine receptors and NMDA receptors have also been detected in postmortem brain examination of a PERM patient.[94] The anti-GlyR-ab demonstrate in vitro evidence of pathogenicity and the patients respond well to immunotherapies such as corticosteroids, IVIg, plasma exchange, and cyclophosphamide.[87, 95]

Anti-GABA receptor encephalitis

The GABA receptors are a class of receptors that respond to the neurotransmitter gamma-aminobutyric acid (GABA), the chief inhibitory neurotransmitter in the vertebrate central nervous system. There are two classes of GABA receptors: $GABA_A$ and $GABA_B$. $GABA_A$ receptors are ligand-gated ion channels (also known as ionotropic receptors), whereas $GABA_B$ receptors are G protein-coupled receptors (also known as metabotropic receptors). Recently autoantibodies have been identified against both $GABA_A$ receptors[96] and $GABA_B$ receptors[97,18,20] in serum and cerebrospinal fluid of paraneoplastic and non-paraneoplastic limbic encephalitis.

The ionotropic $GABA_A$ receptors are pentameric transmembrane receptors that consist of five subunits arranged around a central pore to form chloride ion channels, which mediate most of the inhibitory synaptic transmission in the brain. A plethora of isoforms exist for the $GABA_A$ receptors, which includes six alpha subunits (α_{1-6}), three beta subunits (β_{1-3}), three gamma subunits (γ_{1-3}), as well as a δ, ε, θ, π, and also three rho subunits (ρ_{1-3}), which determine the receptor's agonist affinity, chance of opening, conductance, and other properties.[98,99,100] Each subunit comprises four transmembrane domains with both the N- and C-terminus located extracellularly, usually on the postsynaptic neurons. The majority of $GABA_A$ receptors contain two α subunits, two β subunits, and one γ or δ subunit.

The $GABA_A$ receptor plays a central role in the regulation of brain excitability. Mutations in $GABA_A$ receptor subunits including $\alpha1$, $\beta3$, $\gamma2$, and δ, cause genetic epilepsy syndromes,[101] whereas genetic loss of the $\beta3$ subunit in mice causes seizures as well as learning and memory deficits,[102] therefore the $GABA_A$ receptor can be a strong candidate affected in autoimmune CNS disorders. Autoantibodies against $\beta3$-subunit of $GABA_A$ receptors have recently been reported in two limbic encephalitis patients exhibited with cognitive impairment and multifocal brain MRI abnormalities. Both patients had similar levels of $GABA_A$ receptor antibodies; in addition, one patient also had a low level of anti-LGI1 autoantibodies, and the other also had anti-CASPR2 autoantibodies.[96] Application of the patients' serum to rat hippocampal neuronal cultures specifically decreases both synaptic and surface $GABA_A$ receptors and also selectively reduces miniature inhibitory postsynaptic current (IPSC) amplitude and frequency, without affecting miniature excitatory postsynaptic

currents (EPSCs). These results strongly suggest that the patients' $GABA_A$ receptor autoantibodies play a central role in the patients' symptoms.

The $GABA_B$ receptors are heterodiameric metabotropic receptors of two related seven-transmembrane proteins, $GABA_{B1}$ and $GABA_{B2}$.[103, 104] They inhibit neuronal activity through G-protein-coupled second-messenger systems, which regulate the release of neurotransmitters, the activity of ion channels and adenylyl cyclase. Activation of presynaptic $GABA_B$ receptors inhibit neurotransmitter release by down-regulating high-voltage activated Ca^{2+} channels, whereas postsynaptic $GABA_B$ receptors decrease neuronal excitability by activating a prominent inwardly rectifying K^+ (Kir) conductance that underlies the late inhibitory postsynaptic potentials.[105,106] Autoantibodies against extra-cellular epitope of $GABA_{B1}$ receptors have been reported in several limbic encephalitis patients, often associated with small-cell lung cancer (SCLC) or with concurrent glutamic acid decarboxylase (GAD) autoantibodies, presented with seizures, memory loss and confusion. Some patients also presented with cerebellar ataxia, opsoclonus-myoclonus syndrome (OMS), status epilepticus and anaplastic carcinoid of the thymus.[20,18,97]

Anti-mGluR5 encephalitis

The L-glutamate is a major excitatory neurotransmitter in the CNS and activates both ionotropic and metabotropic glutamate receptors (mGluR). NMDA, AMPA, and Kainate receptors belong to the group of ionotropic glutamate receptors, whereas mGluR1-8 belong to the group of metabotropic glutamate receptors. Ionotropic receptors form an ion channel pore, whereas the metabotropic receptors are G-protein-coupled receptors.

Anti-mGluR5 autoantibodies have recently been reported in two patients with Hodgkin lymphoma (HL) and limbic encephalitis.[107] Antibodies from the patients' serum react with the cell surface and neuropil of hippocampal neurons and also bind the mGluR5 expressed on the surface of transfected HEK-293 cells. Immunoprecipitation and mass spectrometry confirmed binding to the mGluR5, a receptor involved in processes of learning and memory. The reactivity of patients' sera was abolished in brain of mGluR5-null mice, further confirming the antibody specificity to the mGluR5. The anti-mGluR5 autoantibodies associated limbic encephalitis can affect young individuals and respond to immunotherapy and tumor removal.

AIM OF THE STUDY

Intrathecal autoantibodies and oligoclonal immunoglobulins are reported to be the products of clonally expanded plasma cells in the cerebrospinal fluid (CSF) of patients with autoimmune inflammatory disorders, such as multiple sclerosis.[108, 109] Similarly, analysis of IgG-VH repertoire of CSF plasma cells and B cells has revealed over-represented V_H4, V_H1 and V_H5 families and clonally related IgG sequences in several auto-immune inflammatory disorders.[110, 111]

Studies on self-reactive antibodies isolated from CSF and serum of patients with autoimmune encephalitis (AIE) have described the presence of anti-neuronal autoantibodies, such as anti-NMDA receptor, anti-LGI1, anti-AMPA receptor, anti-GAD_{65} and others.[112] However, the temporal course of CSF $CD138^+$ plasma cells/plasmablasts repertoire and source of origin of intrathecal autoantibodies in patients with AIE have not yet been investigated. We presumed that the autoantibodies in the CSF of patients with AIE are also the products of CSF clonally expanded plasma cells/plasmablasts (cePc).

The present study was aimed to examine $CD138^+$ plasma cell repertoire and to re-construct some of the anti-neuronal autoantibodies in the form of recombinant human monoclonal antibodies (rhuMAb) from CSF-derived cePc of patients with AIE. We have established a recombinant antibody platform, which allows us to reconstruct the antigen specificity of single human B cells or plasma cells in the form of recombinant monoclonal antibodies, by FACS sorting of individual CSF plasma cells followed by single cell RT-PCR, cloning and recombinant expression of their paired immunoglobulin heavy and light chain genes. Here, we want to apply this reverse genetic approach to generate a variety of recombinant antibodies specific for targets relevant in AIEs.

Ultimately, we intend to analyze a battery of recombinant monoclonal antibodies derived from various patients with autoimmune encephalitis *in vitro* and *in vivo* to understand the mechanism of their role in disease pathogenesis. The presence of autoantibodies targeting two or more self-antigens in patients with AIE has been reported previously.[96,20] We presume a diversity of potential target antigens for our CSF cePc derived rhuMAb.

MATERIALS & METHODS

Patient's samples

Cerebrospinal fluid (CSF), serum and EDTA-blood samples were collected from autoimmune encephalitis (AIE) patients diagnosed with different kind of anti-neuronal autoantibodies such as anti-NMDA receptor, anti-LGI1, anti-GAD_{65} etc. Samples were collected after signed informed consent in accordance with the institutional protocol from different university hospitals in Germany (i.e. Bonn, Düsseldorf, Münster, etc.). CSF cells were isolated by centrifugation at 300g for 5 min. Supernatants were divided into 1 ml aliquots and cell pellets were resuspended in cell freezing medium (10% DMSO in FBS). Peripheral blood mononucleated cells (PBMC) were prepared from EDTA-blood samples by Biocoll gradient centrifugation according to the manufacturer's instructions (Merck Millipore). All the samples were cryopreserved until use (**Fig. 9A-C**, Pg.36).

Single cell sorting of CSF plasma cells/plasmablasts

For single cell sorting, frozen CSF cells were suspended in RPMI 1640 cell culture medium (Gibco) and centrifuged at 300g for 5 min. Cell pellets were resuspended in 200 µl of FACS buffer (2% FBS in PBS) and incubated with anti-human PerCP-Cy5.5-CD19 (BD Biosciences) and APC-CD138 (Miltenyi biotec) antibodies (each 10 µl) along with 200 nM of DAPI for 30 min on ice. Cells were washed twice by centrifugation at 300g for 5 min to remove the unbound antibodies and resuspended in 200 µl of FACS buffer. Single cell sorting was performed on a MoFlo XDP High Speed Cell Sorter (Beckman-Coulter) at the 'Core Flow Cytometry Facility' at the University Clinic Düsseldorf. Single plasma cells ($CD138^+$) and plasmablasts ($CD19^+/CD138^+$) were sorted, excluding cell duplets, into 96-well PCR plates (Eppendorf) containing 10 µl/well ice-cold cell sorting buffer (0.02% of NP40 and 8 Units of RNaseOut in 10 µl of H_2O; all from Invitrogen). Plates were sealed with AlumaSeal CS Films (Sigma-Aldrich) and immediately frozen on dry ice before storage at −80°C (**Fig. 9D-F**, Pg.36).

Single cell RT-PCR

Immunoglobulin (Ig) heavy and light chain variable region genes were amplified by RT-PCR from single cell cDNA generated by amplification of Ig-mRNA transcripts with gene

specific constant region primers. The single cell RT-PCR of paired IgG-heavy chain variable (VH) and light chain variable (VL) genes were carried out in microtiter plates using Qiagen OneStep RT-PCR kit. In brief; three different master mixes were prepared from the RT-PCR kit with respective primer sets for IgG-VH, Ig-Vκ and Ig-Vλ chains. One third of each single cell lysate was distributed to the respective master mix in a total volume of 20 µl per well. A negative control (without template RNA) was included in every experiment. Reverse transcription was performed for one hour at 50°C followed by 45 cycles of PCR at 94°C for 30s, 52°C (IgH/Igκ/ Igλ) for 30s, 72°C for 1 min. After amplification of 1st round PCR (**Fig. 9G**, Pg.36), samples were stored overnight at 2–8°C, or at –80°C for long-term storage. All PCR products were purified from 1% agarose gel using the QIAquick PCR Purification Kit and subsequently sequenced with the respective constant region primers at GATC Biotech. Clonally expanded paired Ig-variable region gene sequences were identified and selected for recombinant antibody production; either by synthesizing the sequences and sub-cloning (by Life technology, Germany), or by 2nd round PCR with primers containing restriction sites and directly cloning into respective mammalian expression vectors (**Fig. 11**, Pg.39). The sequences of the first and second round PCR primers are presented in **table 2** (Pg.33&34).

Ig-sequence analysis

All the Ig-VH, Ig-Vκ and Ig-Vλ sequences were analyzed by IgBLAST in comparison with GenBank (http://www.ncbi.nlm.nih.gov/igblast/) to identify germline V(D)J gene segments with highest identity. The Ig-VH and Ig-VL complementarity determining region 3 (CDR3) length were determined as indicated in IgBlast by counting the amino acid residues following framework region 3 (FR3) up to the conserved tryptophan-glycine (WG) motif in all JH segments or up to the conserved phenylalanin-glycine (FG) motif in JL segments.[113,114] All sequences were trimmed before FR1 and after J- regions, aligned in separate Ig-VH, Ig-Vκ and Ig-Vλ groups and analyzed using an online multiple alignment program for amino acid and nucleotide sequences called ‘MAFFT version 7’ (http://mafft.cbrc.jp/alignment/server/), for Ig-gene repertoire analysis, phylogenetic tree construction and identification of cePc sequences.

To construct phylogenetic trees of Ig-sequences, 'Newick file format' were generated for Ig-VH, Ig-Vκ and Ig-Vλ sequence groups by using default Neighbor-Joining (NJ) phylogeny method[115] on MAFFT version 7 software. FigTree v1.4.2 software was used to construct unrooted phylogenetic trees. Trees are useful in outlining the phylogenetic relationship among the sequences and Ig-gene repertoire analysis. The branch length and distance between sequences correspond to sequence similarity/dissimilarity, shorter and closer branches relate to a greater sequence similarity.

The external node of a branch represents a 'sequence' or a 'leaf'. Clonally expanded sequences, if identical, aggregate as overlapping 'leaves' on the same node. The bootstrap support values for each branch were calculated based on 100 resamplings of the original data set. High values of the bootstrap (more than 70) represent a better statistical support for the topology in the tree.[116] Functional Ig-gene family repertoire of the CSF plasma cells/plasmablasts isolated from five patients with AIE was calculated from the total number of sequences obtained by single cell RT-PCR. Sequences sharing more than 95% nucleotide identity, having similar or identical CDR3 regions and belonging to same V(D)J germline gene family were considered clonally expanded. Sequences, which appeared to be clonally expanded, were manually cross-checked to confirm the identity among them and accordingly process for cloning and production of recombinant human monoclonal antibodies (rhuMAb).

Cloning

Cloning of the 2nd round PCR products was carried out by restriction enzyme digestion and ligation into the mammalian expression vectors containing respective human Ig-constant regions. The expression vectors contain an IL2 signal peptide sequence, a multiple cloning site upstream of the human Igγ1, Igκ or Igλ2 constant regions and a hEF1-HTLV promotor (**Fig. 8**, Pg.28). Restriction digestion of PCR products and vectors were carried out with respective restriction enzymes, namely EcoRI, NheI and AvrII (all from New England Biolabs), followed by 5'dephosphorylation of the digested vectors using Shrimp Alkaline Phosphatase (New England BioLabs). All the digested products were purified from 1% agarose gel. The ligation reactions between restriction enzymes digested PCR products and corresponding vectors were performed using LigaFast™ Rapid DNA Ligation System

(Promega), overnight at 4°C. One Shot®TOP10 chemically competent E.coli cells were transformed with the ligated products at 42°C following the instruction protocol of the supplier (Invitrogen). The transformed Ig-heavy chain colonies were selected on Zeocin (Invitrogen) agar plates, whereas Ig-light chains colonies (Igκ or Igλ) were selected on Blasticidine (Invitrogen) agar plates. Min-prep plasmid preparations (Qiagen miniprep kit), and subsequent sequencing were carried out on the selected bacterial colonies to confirm the presence of Ig-variable regions inserts. Colonies with confirmed insert sequences were used for maxiprep and an aliquot of the same was frozen as glycerol stock at -80℃ for future use.

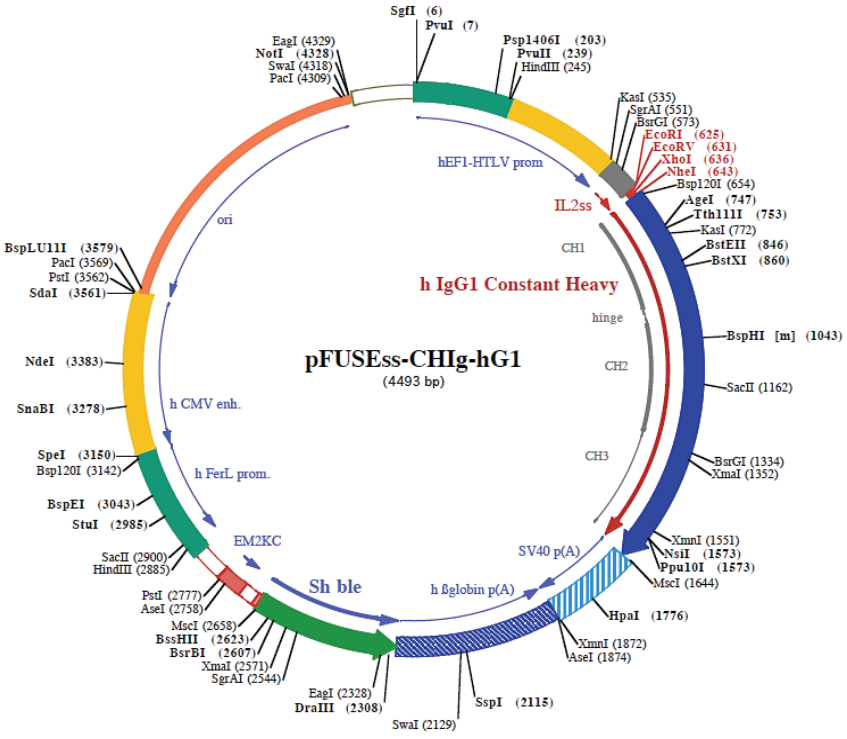

Figure: 8. Schematic map of the mammalian expression vector pFUSEss-CHIg-hG1 containing human Igγ1 constant region (adapted from InVivoGen). The maps of the mammalian expression vectors pFUSE2ss-CLIg containing the constant regions of human Igκ or Igλ2 light chains could be found on InvivoGen website (http://www.invivogen.com/antibody-generation).[125]

Ig-expression vector transfection

FreeStyle™ 293-F cells (Invitrogen) were cultured in TC-175 cm^2 flask (Greiner Bio-one) under standard conditions in Gibco® RPMI 1640 medium supplemented with 10% heat-inactivated fetal calf serum (FCS), 100 µg/ml streptomycin, 100 U/ml penicillin (all from Invitrogen). Co-transfections of Ig-heavy chain and matching Ig-light chain expression vectors (20 µg each/flask) were performed using linear polyethylenimine (PEI) as a transfection reagent (Polysciences, Inc.).[124] In brief; 1:3 concentration ratio of plasmids:PEI were mixed in 500 µl Opti-MEM reduced serum media (Invitrogen) 30 min at RT, and subsequently incubated on 90% confluent cells in a total volume of 20 ml medium/flask for 24 hrs. The transfection medium was replaced with antibody harvesting medium containing RPMI 1640 supplemented with 1X Nutridoma-SP (Roche), 100 µg/ml streptomycin, 100 U/ml penicillin. The antibody harvesting medium was collected after one week of incubation, and cells were either re-incubated with fresh harvesting medium or stored in cell freezing medium (10% DMSO in FBS) at -80°C for future use. Stable transfected cells were obtained for at least three subcultures in the presence of 500 µg/ml Zeocin and 10 µg/ml Blasticidin antibiotics (all from Invitrogen).

Antibody purification

The human recombinant IgG1 antibodies were purified from harvested supernatants either by using HiTrap Protein G HP columns (GE Healthcare) on FPLC system (ÄKTA Prime), or by using the Magne™ Protein G Beads (Promega). In brief: harvested supernatants were centrifuged at 8000g for 10 min, filtered using 0.2µm vacuum filter (Sarstedt) and adjusted to pH 7.4 using a 1M-Tris-HCl buffer (pH 8.8). The supernatants were either circulated on protein G HP columns (columns pre-equilibrated with 20mM-Tris-HCl; pH 7.4), or incubated with Magne protein G beads overnight at 4°C. The protein G HP column bound antibodies were eluted using a 0.1M-Glycine-HCl buffer (pH 2.7) on FPLC system, whereas Magne protein G beads bound antibodies were first separated from supernatants on a magnetic stand, washed with PBS, and then eluted with 0.1M-Glycine-HCl buffer (pH 2.7). Eluted antibodies were adjusted to pH 7.4 with 1M-Tris-HCl buffer (pH 8.8). Buffer exchange was performed with PBS either by dialysis using 10K MWCO Slide-A-Lyzer

Dialysis Cassettes (Thermo scientific), or by using 30K Amicon Ultra-15 centrifugal Filter Units (Merck Millipore). The protein concentrations of purified antibodies were determined by BC assay kit (Uptima).

The purity of the eluted recombinant monoclonal antibodies was determined by SDS-PAGE. Semi denatured samples were prepared by mixing 5 µg of eluted antibodies with 1X-NuPAGE sample reducing agent (Invitrogen), heated 10 min at 60°C, and loaded on 4-16 % Precise™ Protein gel (Thermo scientific), along with Novex Sharp pre-stained protein standard (Invitrogen). The samples were run in NuPage-MOPS SDS running buffer (Invitrogen) 30 min at 120 V and subsequently stained with Gel code™ Blue stain reagent (Thermo Scientific) to visualize the complete antibody bands along with Ig-heavy and light chain bands. Purified recombinant antibodies were aliquoted with and without 0.05% sodium azide and stored at -80°C.

Antigen expression vectors

The ORF Gateway™ entry clone vectors (pENTR(tm)221), containing the gene of choice, such as human LGI1 (NM_005097.2), and human GAD2 (NM_000818.2) sequences were bought from Invitrogen, along with a mammalian expression vector kit 'Vivid Colors™ pcDNA™6.2/EmGFPG.Bsd/V5-DEST' all supplied in E. coli host cells. Plasmids were purified from the respective clones as instructed by the supplier.

Mammalian expression vectors expressing desired gene were generated by LR recombination reactions between Gateway entry vectors containing the gene of choice and the mammalian expression vector. The recombination reactions were performed by using LR Clonase II enzyme mix kit (Invitrogen) and subsequently transformed in TOP10 E.coli cells following the instruction protocol of the supplier. Sequencing of the recombinant expression vectors was carried out with T7 promoter primer to confirm the presence of gene of choice.

Mammalian expression vectors containing rat NR1/1a (NM_017010.2) and rat NR2B (NM_012574.1) subunit sequences were obtained as a gift from professor Nikolaj Kloecker, Institute of Neuro- and Sensory Physiology, Heinrich Heine University, Düsseldorf.

Immunocytochemistry (ICC)

HEK-293 cells grown on 0.05 % Poly-D-lysine (Sigma-Aldrich) coated coverslips in six well plates (Greiner Bio-one) were transfected with mammalian expression vectors containing gene of choice, such as LGI1, GAD_{65} etc., using lipofectamine 2000 (Invitrogen) as transfection reagent. Co-transfections were carried out with expression vectors containing rat-NR1/1a and NR2B subunits in equimolar ratios, to generate functional NMDA receptor. The functional NMDA receptor expressing cells were grown in the presence of 500µM ketamine (an inhibitor of NMDA receptor; Sigma-Aldrich) to prevent cell death.[5] A control expression vector containing eGFP was included in each transfection. The HEK-293 cells expressing LGI1 were incubated with 100 ng/ml Brefeldin-A (Sigma-Aldrich) to inhibit protein secretion for 1hr before fixation.[38]

Immunocytochemistry was performed to determine the reactivity of recombinant monoclonal antibodies to the target antigens expressed by the transgenic cells. In brief: cells were fixed in 4% ice-cold paraformaldehyde (PFA) and blocked with 5% donkey serum. When tested for intracellular antigens such as GAD_{65} and LGI1 (Brefeldin-A treated), cells were permeabilized with 0.2% Triton X-100 (Sigma-Aldrich), otherwise directly incubated with respective recombinant monoclonal antibodies (10 µg/ml) overnight at 4°C. Cells were washed with 0.2% Tween 20 (T20-PBS) and incubated with 1:1000 diluted Cy3-affiniPure $F(ab')_2$ donkey anti-human secondary antibodies (Jackson ImmunoResearch), for 2 hrs at RT. Stained cells were washed with T20-PBS containing 300 nM DAPI, before mounting on the glass slides using Immu-Mount (Thermo Scientific). Commercially available antibodies such as anti-GAD_{65} (abcam), anti-LGI1 (abcam), anti-NR1/1a (Merck Millipore) and anti-NR2B (abcam) were used as positive controls for the respective immunostaining. A chimeric human antibody 818C5 (purified in similar conditions as rhuMAb) specific for a known irrelevant antigen (myelin oligodendrocyte glycoprotein, MOG) was used as a negative control. Pictures of immunostained cells were acquired with 60 x oil-immersion objective of the Olympus-BX51 fluorescence microscope.

Immunoprecipitations (IP)

Female Wistar rats were anesthetized with Isoflurane (Actavis), decapitated and the whole brain was instantly snap-frozen in liquid nitrogen. A frozen marmoset brain was received

from animal house, Heinrich Heine University, Düsseldorf. Frozen human brain tissue samples were obtained from different institutional brain banks. Homogenization of the frozen brains was performed using a buffer containing 320 mM sucrose, 20 mM Tris-HCl pH 7.4, 1 mM IAA (2-Iodoacetamide), 1 mM EDTA, 1 mM PMSF (phenylmethanesulfonylfluoride), complete Roche proteinase inhibitor cocktail tablets (without EDTA) and a glass pestle. Cell debris was removed by a brief centrifugation at 1000g for 10 min at 4°C before total membrane fractions were prepared by ultracentrifugation at 275000g for 20 min at 4°C. Protein concentrations were determined by BC assay kit (Uptima).

Solubilization of membrane proteins was carried out at 4°C for 30 min using 1% dodecanoylsucrose (DDS) and 150 mM NaCl (for NMDAR fraction: 1 % DDS, 1 % deoxycholate and 200 mM NaCl) in 20 mM Tris-HCl pH 7.4, 1 mM IAA, 1 mM EDTA, 1 mM PMSF, complete Roche proteinase inhibitor cocktail tablets without EDTA. Non-solubilized matter was pelleted at 125000g for 15 min at 4°C and the supernatant was prepared for the immunoprecipitations (IPs) by pre-clearing for 2 hr at 4°C with non-coupled Dynabeads.

IPs were performed using recombinant human monoclonal antibodies overnight at 4°C under constant agitation with 5 μg of antibodies covalently coupled with Dynabeads via DMP, washed 4x 10 min before elution with 1x lithium dodecyl sulfate (LDS) sample buffer.

Western blot

The LDS (lithium dodecyl sulfate) eluted IP samples were supplemented with 100 mM DTT and reduced at 37°C for 15 min. Samples were run on 4-20% reducing SDS-PAGE gels, blotted to PVDF membrane and blocked with 5% BSA. Primary antibodies (abcam rabbit anti-LGI1; abcam rabbit anti-GAD_{65}; Millipore rabbit anti-NR1) were incubated overnight at 4°C followed by subsequent PBS-T washes for 1 hr. A Santa Cruz goat-anti-rabbit IgG HRP (sc-2004) antibody was used as secondary antibody. Detection was carried out using a GE Healthcare ECL substrate.

First round PCR primers		
IgG-heavy chain forward primers	V_H17-F	CAG GTG CAG CTG GTG CA(AG) TCT GG
	V_H2-F	CAG ATC ACC TTG AAG GAG TCT GG
	V_H35-F	GAG GTG CAG CTG GTG (GC)AG TCT GG
	V_H3a-F	GAG GTG CAG CTG (GT)TG GAG TCT GG
	V_H4-F	CAG GTG CAG CTG CAG GAG TCG GG
	V_H4a-F	CAG GTG CAG CTA CAG CAG TGG GG
	V_H6-F	CAG GTA CAG CTG CAG CAG TCA GG
IgG-heavy chain reverse primer	$C_H\gamma1$	GTT GTC CAC CTT GGT GTT GCT GG
Ig-kappa chain forward primers	Vk1-F	GAC ATC CRG DTG ACC CAG TCT CC
	Vk36-F	GAA ATT GTR WTG ACR CAG TCT CC
	Vk2346-F	GAT ATT GTG MTG ACB CAG WCT CC
	Vk5-F	GAA ACG ACA CTC ACG CAG TCT CC
Ig-kappa chain reverse primer	Ck1	ACACTCTCCCCTGTTGAAGCTCTT
Ig-lambda chain forward primers	Vλ1-F	GAG TCT GTS BTG ACG CAG CCG CC
	Vλ3a-F	TCC TAT GWG CTG ACW CAG CCA C
	Vλ38-F	TCC TAT GAG CTG AYR CAG CYA CC
	Vλ1459-F	CAG CCT GTG CTG ACT CAR YC
	Vλ78-F	CAG DCT GTG GTG ACY CAG GAG CC
	Vλ15910-F	CAG CCW GKG CTG ACT CAG CCM CC
	Vλ3B-F	TCC TCT GAG CTG AST CAG GAS CC
	Vλ2-F	CAG TCT GCC CTG AYT CAG CCT
	Vλ6-F	AAT TTT ATG CTG ACT CAG CCC
Ig-lambda chain reverse primer	Cλ1	TGAACATTCTGTAGGGGCCAC

- The variable region primers are from Phage display chaper 9.8[126]
- Constant region primers $C_H\gamma1$, Ck1 and Cλ1 are adapted from Owens et al.[127]

Table 2. Primer sequences

Second round PCR primers with restriction sites		
IgG-heavy chain forward primers	5'EcoRI-V_H1	GTC ACG AAT TCG CAG GTG CAG CTG GTG CAG
	5'EcoRI-V_H1/5	GTC ACG AAT TCG GAG GTG CAG CTG GTG CAG
	5'EcoRI-V_H3	GTC ACG AAT TCG GAG GTG CAG CTG GTG GAG
	5'EcoRI-V_H4	GTC ACG AAT TCG CAG GTG CAG CTG CAG GAG
	5'EcoRI-V_H3-23	GTC ACG AAT TCG GAG GTG CAG CTG TTG GAG
	5'EcoRI-V_H4-34	GTC ACG AAT TCG CAG GTG CAG CTA CAG CAG
IgG-heavy chain reverse primer	3'NheI–J_H1/2	CTT GGT GCT AGC GAG GAG ACG GTG ACC AG
	3'NheI–J_H3	CTT GGT GCT AGC GAA GAG ACG GTG ACC ATT
	3'NheI-J_H4/5	CTT GGT GCT AGC TGA GGA GAC GGT GAC CAG
	3'NheI–J_H6	CTT GGT GCT AGC TGA GGA GAC GGT GAC CGT G
Ig-kappa chain forward primers	5'EcoRI-Vk1-5	TC ACG AAT TCA GAC ATC CAG ATG ACC CAG TC
	5'EcoRI-Vk 1-9	TC ACG AAT TCA GAC ATC CAG TTG ACC CAG TCT
	5'EcoRI-Vk1D-43	TC ACG AAT TCA GCC ATC CGG ATG ACC CAG TC
	5'EcoRI-Vk2-24	TC ACG AAT TCA GAT ATT GTG ATG ACC CAG AC
	5'EcoRI-Vk2-28	TC ACG AAT TCA GAT ATT GTG ATG ACT CAG TC
	5'EcoRI-Vk3-11	TC ACG AAT TCA GAA ATT C
	5'EcoRI-Vk3-15	TC ACG AAT TCA GAA ATA GTG ATG ACG CAG TC
	5'EcoRI-Vk3-20	TC ACG AAT TCA GAA ATT GTG TTG ACG CAG TCT
	5'EcoRI-Vk4-1	TC ACG AAT TCA GAC ATC GTG ATG ACC CAG TC
Ig-kappa chain reverse primer	3'BsiWI-Jk1/2/4	AGC CAC CGT ACG TTT GAT YTC CAC CTT GGT C
	3'BsiWI-Jk2	AGC CAC CGT ACG TTT GAT CTC CAG CTT GGT C
	3'BsiWI-Jk3	AGC CAC CGT ACG TTT GAT ATC CAC TTT GGT C
	3'BsiWI-Jk5	AGC CAC CGT ACG TTT AAT CTC CAG TCG TGT C
Ig-lambda chain forward primers	5'EcoRI-Vλ1	GTC ACG AAT TCG CAG TCT GTG CTG ACK CAG
	5'EcoRI-Vλ2	GTC ACG AAT TCG CAG TCT GCC CTG ACT CAG
	5'EcoRI-Vλ3	GTC ACG AAT TCG TCC TAT GAG CTG ACW CAG
	5'EcoRI-Vλ4/5	GTC ACG AAT TCG CAG CYT GTG CTG ACT CA
	5'EcoRI-Vλ6	GTC ACG AAT TCG AAT TTT ATG CTG ACT CAG
	5'EcoRI-Vλ7/8	GTC ACG AAT TCG CAG RCT GTG GTG ACY CAG
Ig-lambda chain reverse primer	3' AvrII-Jλ1/6	GC TGA CCT AGG TAG GAC GGT SAC
	3' AvrII-Jλ4	GC TGA CCT AGG TAA AAT GAT CAG
	3' AvrII-Jλ7	GC TGA CCT AGG GAG GYC GGT CAG

- Restriction sites are underlined.

Table 2. Primer sequences continued.

RESULTS

Strategy to generate recombinant human monoclonal antibodies

To reconstruct intrathecal autoantibodies from patients with autoimmune encephalitis (AIE), we have established a method, which allows Ig-gene repertoire analysis and production of human recombinant monoclonal antibodies of the same specificity *in vitro* from single cells. Using FACS sorting of individual CSF plasma cells followed by single cell RT-PCR, cloning and recombinant expression of paired immunoglobulin heavy and light chain genes, we successfully rebuilt intrathecal antibody responses of patients with AIE (**Fig. 9,** Pg.36).

Single cell sorting

For the analysis of Ig-gene repertoire and clonally expanded plasma cells (cePc), we FACS sorted a total of 584 individual CSF plasma cells ($CD138^+$) and plasmablasts ($CD19^+CD138^+$) from five patients with AIE into 96 well plates. The patients were prediagnosed with different kind of anti-neuronal autoantibodies, such as anti-NMDA receptor (SSM), anti-LGI1 (GKD), anti-GAD_{65} (JMB), and two with anti-CASPR2 (KKM & BRM). As a negative control, no cell was sorted into five wells (**Fig. 10,** Pg.37).

Single cell RT-PCR

Expressed IgG-heavy chain variable (VH) and Igκ or Igλ light chain variable (VL) genes were amplified separately by RT-PCR from single cell cDNA generated by priming of Ig-mRNA transcripts with gene specific constant region primers. The 1^{st} round PCR was performed with forward mixed-primers specific for the FR1-region of different Ig-V families, and a reverse primer specific for the respective IgH, Igκ or Igλ constant regions. All RT-PCR amplicons were purified from 1% agarose gel and subsequently sequenced (**Fig. 9**, Pg.36 **& Fig. 11**, Pg.39). Out of 584 individual $CD138^+$ plasma cells/plasmablasts sorted, sequencing of PCR products produced 508 clearly readable IgG-heavy chain variable region sequences, resulting in an efficiency of 86.98%. Sequencing of light chain PCR products produced 305 Ig-Vκ and 114 Ig-Vλ sequences.

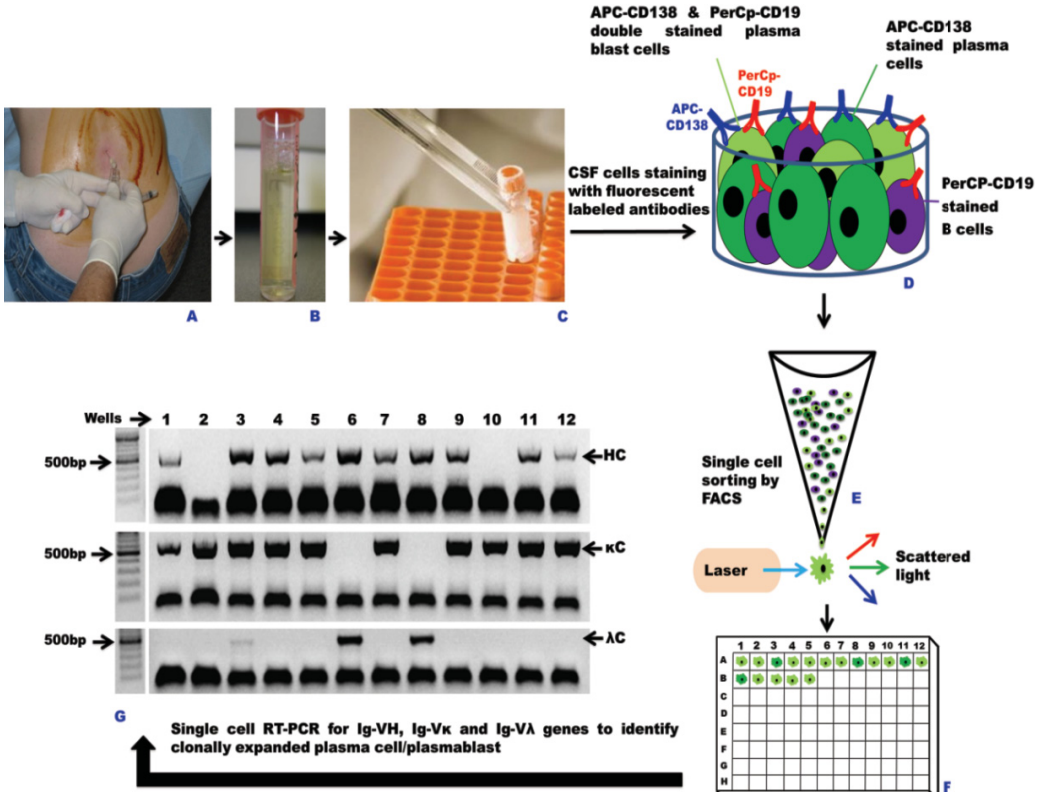

Figure: 9. Schematic presentation of human cerebrospinal fluid (CSF) cells processes.
The cells isolated from the CSF samples of patients with AIE were stained with PerCPg.CD19 and APC-CD138 fluorescent labeled antibodies (**A-D**). Single plasma cells ($CD138^+$) and plasmablast ($CD138^+/CD19^+$) were collected in microtitre plates by FACS (**E-F**). The subsequent single cell RT-PCR were performed for Ig-VH, Ig-Vκ and Ig-Vλ genes (**G**), to identify clonally expanded paired Ig-heavy and light chain variable regions for the production of recombinant human monoclonal antibodies (rhuMAb).

Repertoire analysis of CSF plasma cells/plasmablasts

The CSF $CD138^+$ plasma cells/plasmablasts repertoires were examined from the samples of five patients with AIE. All the Ig-VH, Ig-Vκ and Ig-Vλ sequences were analyzed by IgBLAST in comparison with the IMGT germline gene entry (http://www.ncbi.nlm.nih.gov/igblast/) to identify closest germline V(D)J gene segments

with highest identity. The Ig-VH and Ig-VL complementarity determining region 3 (CDR3) length was determined as indicated in IgBlast by counting the amino acid residues following framework region 3 (FR3) up to the conserved tryptophan-glycine (WG) motif in all JH segments or up to the conserved phenylalanin-glycine (FG) motif in JL segments (**Table 5a&b**, Pg.44).[113,114] All the sequences were trimmed before FR1 and after J- regions, aligned in individual Ig-VH, Ig-Vκ and Ig-Vλ groups. Sequences were analyzed using an online multiple alignment program for amino acid and nucleotide sequences called 'MAFFT version 7' (http://mafft.cbrc.jp/alignment/server/) to analyze Ig-genes repertoires, phylogenetic tree construction and to identify clonally expanded plasma cells/plasmablasts (cePc) sequences.

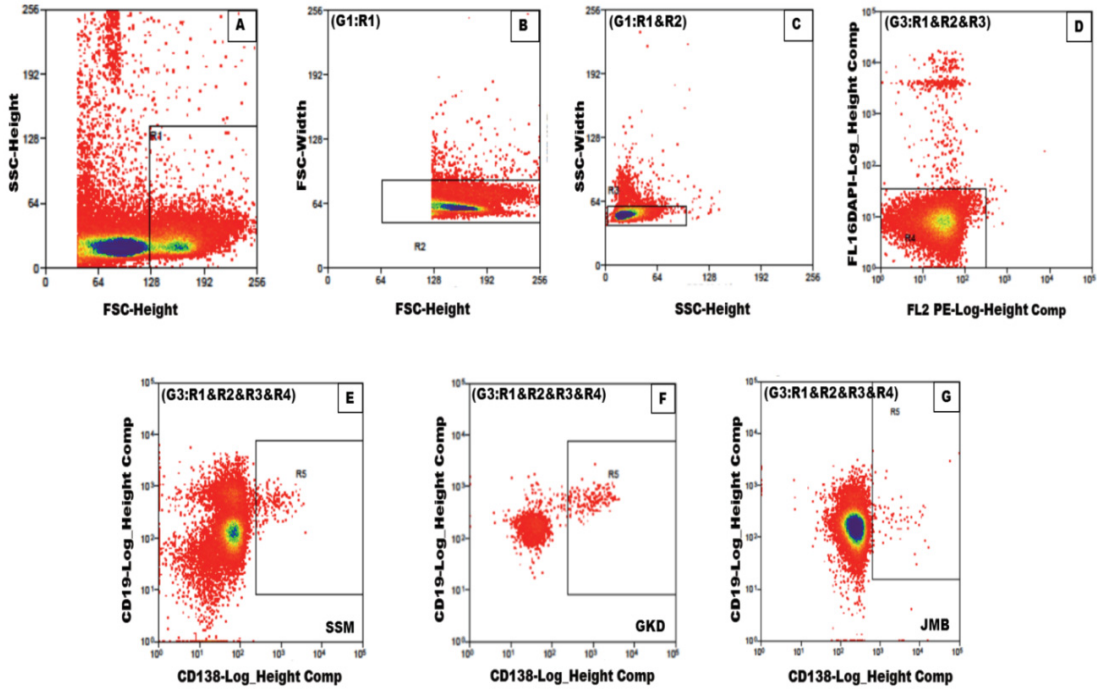

Figure: 10. Isolation of single plasma cell (CD138$^+$) and plasmablast (CD19$^+$/CD138$^+$) by FACS. In brief: CSF cells were incubated with a mixture of fluorescent labeled antibodies to human CD19 and CD138 antigens. Total living cells were selected by SSC vs FSC light scattering (**A; R1**); cell duplicates or larger aggregates were excluded (**B&C; R2&R3**). The living cells were selected excluding DAPI positive dead cells for the collection of single plasma cell and plasmablast (**D; R4**). Single plasma cell (CD138$^+$) and plasmablast (CD19$^+$/CD138$^+$) were collected in 96 well plates from the CSF of five patients with AIE, e.g. SSM, GKD, JMB (**E, F & G; R5**) and two others (KKM & BRM, not shown).

Unrooted phylogenetic trees were constructed separately for Ig-VH, Ig-Vκ and Ig-Vλ sequence groups to identify the genetically similar or identical sequences and representation of Ig-families in the CSF plasma cells/plasmablasts. The statistical topology of the phylogenetic trees was supported by calculating the bootstrap values for each branch on the tree, based on 100 resamplings of the original data set. High values of the bootstrap (more than 70) represent a better statistical support for the topology in the tree.[116]

No.	Patients (pre-diagnosed autoantibody)	Number of IgG-HC sequences	IgG-VH family representation in individual patient					Matching Figures
			V_H1 family	V_H3 family	V_H4 family	V_H5 family	V_H7 family	
1	GKD (anti-LGI1)	86	24 seq. (27.9%)	34 seq. (39.5%)	27 seq. (31.3%)	1 seq. (1.16%)	nf*	Fig.12 (p-41)
2	SSM (anti-NMDAR)	37	2 seq. (5.4%)	27 seq. (72.9%)	5 seq. (13.5%)	3 seq. (8.1%)	nf*	Fig.13 (p-42)
3	JMB (anti-GAD_{65})	42	29 seq. (69.0%)	7 seq. (16.6%)	3 seq. (7.1%)	3 seq. (7.1%)	nf*	Fig.13 (p-42)
4	KKM (anti-CASPR2	161	37 seq. (22.9%)	91 seq. (56.5%)	21 seq. (13.0%)	8 seq. (4.9%)	4 seq. (2.4%)	Fig.13 (p-42)
5	BRM (anti-CASPR2)	182	63 seq. (34.6%)	68 seq. (37.3%)	43 seq. (23.6%)	8 seq. (4.3%)	nf*	Fig.13 (p-42)
	Total	508	155 seq. (30.5%)	227 seq. (44.6%)	99 seq. (19.4%)	23 seq. (4.5%)	4 seq. (0.7%)	

Table 3a. Repertoire analysis of CSF plasma cells/plasmablasts IgG-VH sequences of five AIE patients.

nf*(not found)

	Total No. of Seq.	Cumulative Ig-families representation							Matching Figures
IgG-VH	508	V_H1 155 seq. (30.5%)	V_H3 227 seq. (44.6%)	V_H4 99 seq. (19.4%)	V_H5 23 seq. (4.5%)	V_H7 4 seq. (0.7%)			Fig.19 (p-57)
Ig-Vk	305	V_k1 135 seq. (44.2%)	V_k2 29 seq. (9.5%)	V_k3 124 seq. (40.6%)	V_k4 16 seq. (5.2%)	V_k5 01 seq. (0.3%)			Fig.20 (p-58)
Ig-Vλ	114	$V_λ1$ 17 seq. (14.9%)	$V_λ2$ 32 seq. (28.0%)	$V_λ3$ 56 seq. (49.1%)	$V_λ6$ 04 seq. (3.5%)	$V_λ7$ 02 seq. (1.7%)	$V_λ8$ 02 seq. (1.7%)	$V_λ9$ 01 seq. (0.8%)	Fig.21 (p-59)

Table 3b. Repertoire analysis of cumulative Ig-VH, Ig-Vκ and Ig-Vλ sequences from the CSF plasma cells/plasmablasts of five AIE patients.

***nf (not found)**

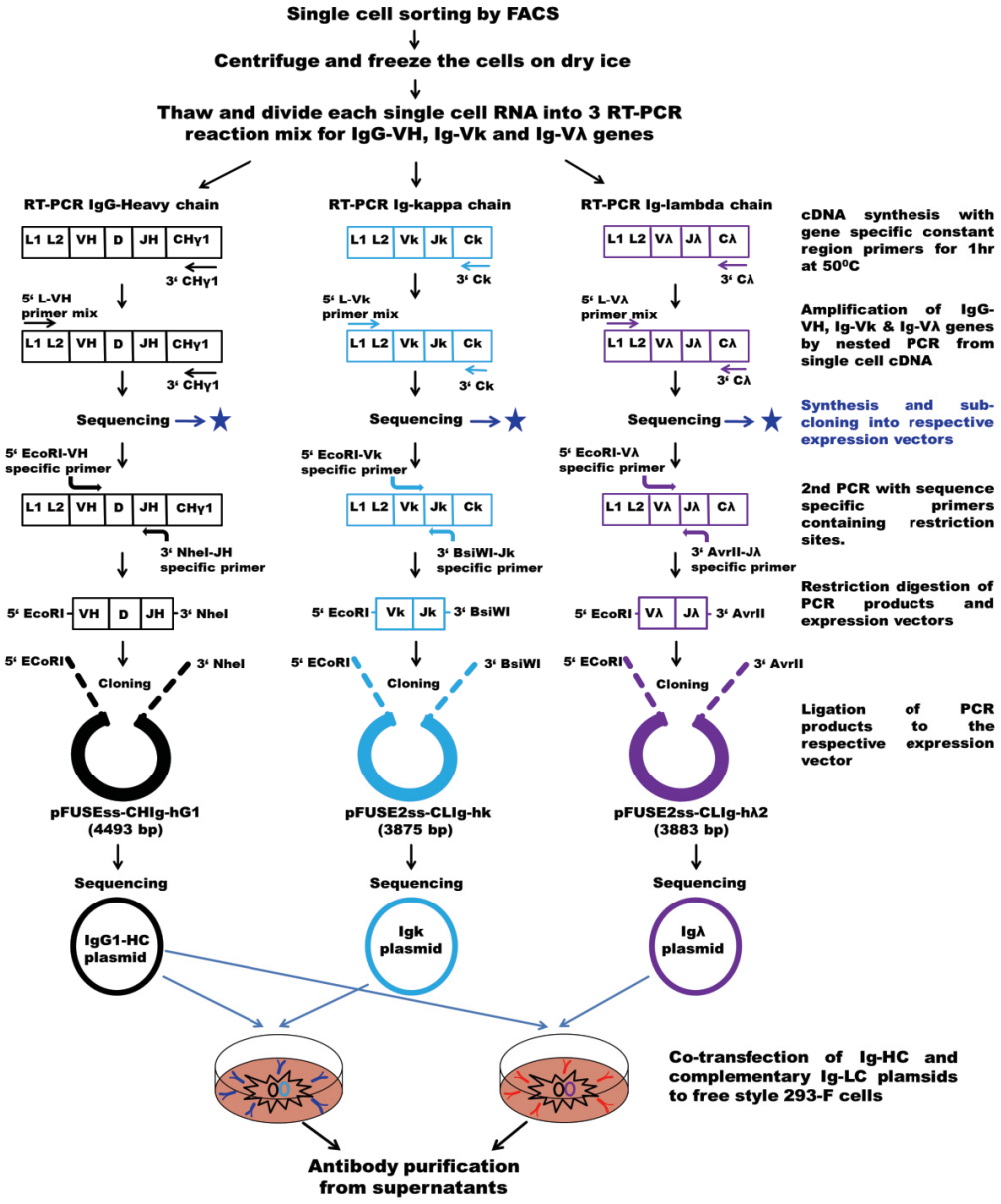

Figure: 11. Strategy to generate recombinant human monoclonal antibodies (rhuMAb).
Ig-heavy and light chain genes were amplified by nested RT-PCR from single cell cDNA generated by amplification with gene specific constant region primers. The cDNA generated from single cells were used as template for 1st round PCR with forward mixed-primers specific for the FR1-region of different Ig-V families, and a reverse primer specific for the respective IgH, Igκ or Igλ constant regions. All the RT-PCR amplicons were purified and subsequently sequenced. Clonally expanded Ig-variable region sequences were identified and selected for recombinant monoclonal antibody production; either by synthesizing the sequences and sub-cloning, or by 2nd round PCR with primers containing restriction sites and directly cloning into the respective mammalian expression vectors. For recombinant antibody production, paired Ig-heavy and light chain plasmids were co-transfected into free style 293-F cells and secreted antibodies were purified from the supernatants.

Single cell RT-PCR of IgG-VH, Ig-Vκ and Ig-Vλ genes revealed 89.5% Igκ and 96% Igλ light chains paired with IgG heavy chain in the CSF plasma cells/plasmablasts of the five AIE subjects tested.

Sequence analysis of RT-PCR amplicons revealed a skewed usage of Ig-variable region genes. The CSF plasma cells/plasmablasts of all five AIE patients represented V_H3, V_H1, V_H4 and V_H5 Ig-heavy chain variable region gene families (**Table 3a&b**, Pg.38).

Patients	GKD (Anti-LGI1)	SSM (Anti-NMDAR)	JMB (Anti-GAD_{65})	KKM (Anti-CASPR2)	BRM (Anti-CASPR2)	Total
cePc IgG-VH clones	7	7	2	21	20	57
No. of cePc sequences	31 seq. (36.0%)	17 seq. (45.9%)	7 seq. (16.6%)	57 seq. (35.4%)	68 seq. (37.3%)	180 seq. (35.4%)

Table 4a. Repertoire analysis of CSF cePc of five AIE patients.

	cePc clones	cePc sequences	Cumulative cePc Ig-family representation						
IgG-VH	57	180 seq. (35.4%)	V_H1 67 seq. (13.1%)	V_H3 65 seq. (12.7%)	V_H4 41 seq. (8.0%)	V_H5 5 seq. (0.9%)	V_H7 2 seq. (0.3%)		
IgG-Vκ	46	118 seq. (38.6%)	Vκ1 59 seq. (19.3%)	Vκ2 6 seq. (1.9%)	Vκ3 47 seq. (15.4%)	Vκ4 6 seq. (1.9%)	Vκ5 *nf		
IgG-Vλ	21	65 seq. (57.0%)	Vλ1 05 seq. (4.3%)	Vλ2 19 seq. (16.6%)	Vλ3 37 seq. (32.4%)	Vλ6 02 seq. (1.7%)	Vλ7 *nf	Vλ8 02 seq. (1.7%)	Vλ9 *nf

Table 4b. Repertoire analysis of cumulative cePc sequences from the CSF plasma cells/plasmablasts of five AIE patients.

*nf (not found)

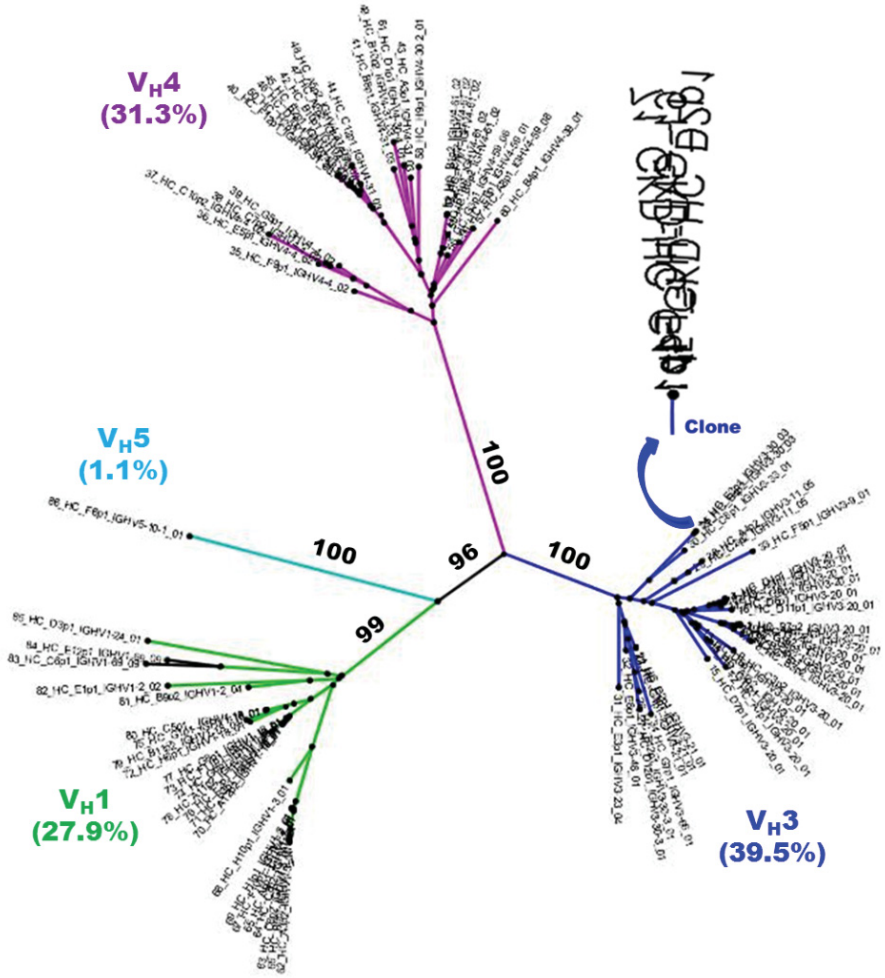

Figure: 12. Unrooted phylogenetic tree of IgG heavy chain variable region sequences derived from the CSF plasma cells /plasmablasts of GKD.

The tree representing the IgG-VH gene family repertoire calculated from 86 sequences. The branch length and distance between sequences correspond to sequence similarity/dissimilarity, shorter and closer branches relate to a greater sequence similarity. Sequences belonging to one family share similarities and group together. Thus, each colored branch of the tree represents a single VH family. The external node of a branch represents a 'leaf' or a 'sequence'. Clonally expanded sequences, if identical, aggregate as overlapping 'leaves' on the same external node (**inset**). The bootstrap support values for each branch on the tree were calculated based on 100 resampling of the original data set.

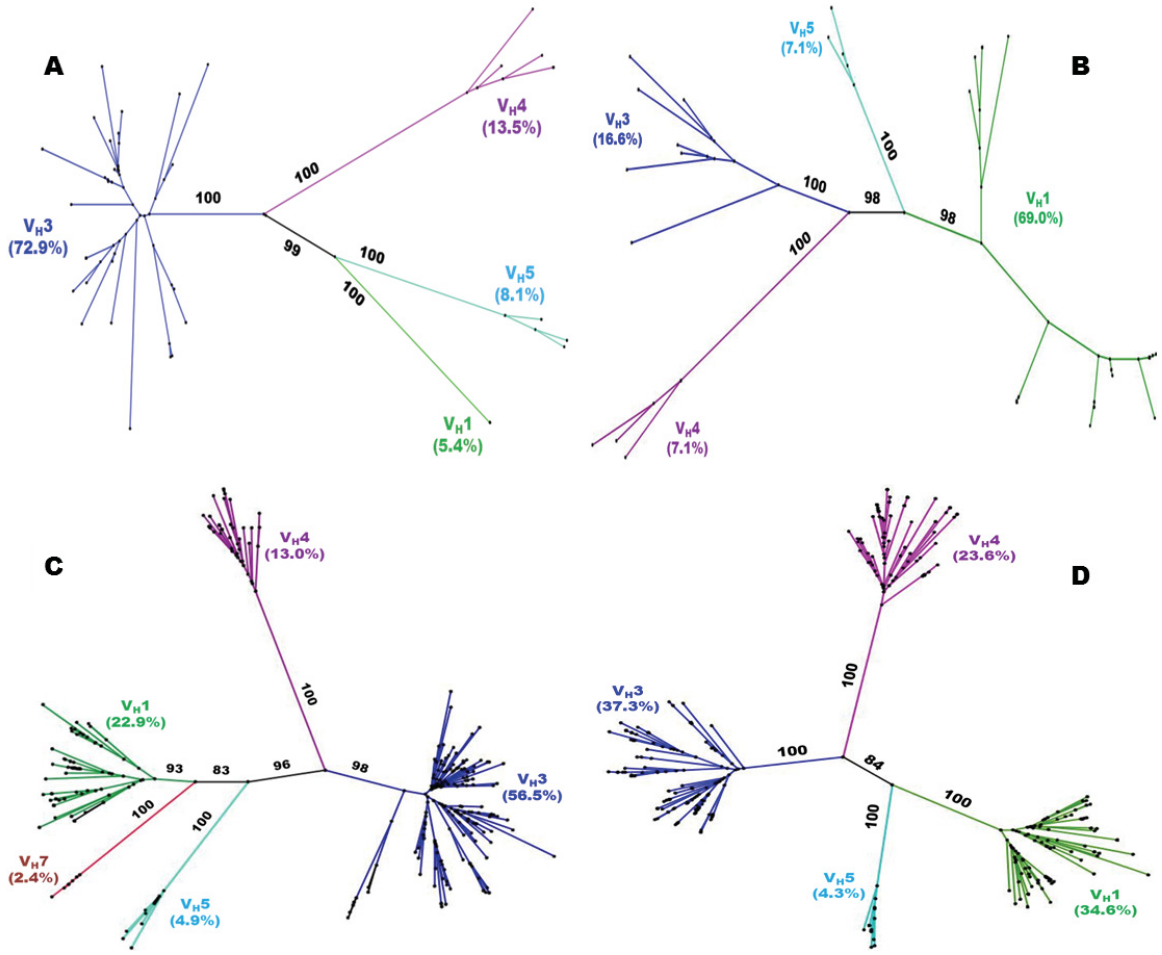

Figure: 13. Unrooted phylogenetic trees of IgG heavy chain variable region sequences derived from the CSF plasma cells /plasmablasts of patients with AIE.

The trees are representing IgG-VH gene family repertoire of SSM (**A**), JMB (**B**), KKM (**C**) and BRM (**D**) patients. The branch length and distance between sequences correspond to sequence similarity/dissimilarity, shorter and closer branches relate to a greater sequence similarity. Each colored branch of the tree represents a single VH family. The external node of a branch represents a 'leaf' or a 'sequence' (**Fig. 12**, Pg.41). For the clarity of the pictures 'sequences' or 'leaves' on the external nodes are not shown. The bootstrap support values for each branch on the tree were calculated based on 100 resampling of the original data set.

Repertoire analysis of IgG-VH amplicons from the CSF plasma cells/plasmablasts of a patient pre-diagnosed with anti-LGI1 autoantibody (GKD) revealed mostly IgG heavy chain amplicons belonging to the V_H3 gene family (39.5%), followed by V_H4 (31.3%), V_H1 (27.9%) and V_H5 (1.1%) families (**Table 3a**, Pg.38 and **Fig. 12**, Pg.41).

Two patients (KKM and BRM), pre-diagnosed with anti-CASPR2 autoantibodies also had a high representation of V_H3 family in the CSF plasma cells/plasmablasts followed by V_H1, V_H4, and V_H5 families. Similarly, V_H3 family (72.9%) was also mostly represented in the CSF of a patient pre-diagnosed with anti-NMDA receptor antibody (SSM) followed by V_H4 (13.5%), V_H5 (8.1%); however, the V_H1 family (5.4%) was found under-represented (**Table 3a**, Pg.38 and **Fig. 13**, Pg.42). On the other hand, a patient pre-diagnosed with anti-GAD_{65} autoantibodies (JMB) had a high representation of the V_H1 family (69.0%) followed by V_H3 (16.6%). Whereas, the V_H4 and the V_H5 families were found equally represented. The V_H7 family was least represented and found only in one patient pre-diagnosed with anti-CASPR2 autoantibodies (**Table 3a**, Pg.38 and **Fig. 13**, Pg.42).

Cumulative sequence analysis of IgG-VH (508 seq.), Ig-Vκ (305 seq.) and Ig-Vλ (114 seq.) amplicons from the CSF plasma cells/plasmablasts of five patients revealed mostly IgG heavy chain amplicons belonging to the V_H3 gene family (44.6%), followed by V_H1 (30.5%), V_H4 (19.4%), V_H5 (4.5%) and V_H7 (0.7%) families (**Table 3b**, Pg.38 and **Fig. 19**, Pg.57). Light chain amplicons were clearly dominated by Ig-Vκ (72.7%) as compared to Ig-Vλ gene segments (27.2%). Among those, Vκ1 gene segments were most commonly used (44.2%), followed by Vκ3 (40.6%), Vκ2 (9.5%), Vκ4 (5.2%) and Vκ5 (0.3%) families (**Table 3b**, Pg.38 and **Fig. 20**, Pg.58). The Ig-Vλ gene segments were diversified belonging to seven families, dominated by Vλ3 (49.1%), followed by Vλ2 (28.0%), Vλ1 (14.9%), Vλ6 (3.5%), Vλ7 (1.7%), Vλ8 (1.7%) and Vλ9 (0.8%) families (**Table 3b**, Pg.38 and **Fig. 21**, Pg.59).

Name of the rebuilt IgG-VH clones	Corresponding IgG-VH family	IgG-VH seq. belonging to respective clones	Amino acids sequence of CDR3 region of corresponding IgG-VH clones
GKD1-HC	VH3	6	DPEIAAAGSHYYYYGMDVWG
GKD2-HC	VH3	3	VKAAVAGTVDYWG
GKD3-HC*	VH1	5	SPTVGGTIRGMDVWG
GKD4-HC*	VH4	3	ENDLDGLDVWG
GKD5-HC*	VH4	5	DRGNWNSRSSFDIWG
GKD6-HC	VH4	4	GDYDILTGYFFFDYWG
GKD7-HC	VH1	5	IMVRGVIEAMDVWG
SSM1-VH	VH3	2	CAKVLYYDSSGFGYYGMDVWG
SSM2-VH	VH4	3	CARDTGYETRFDLWG
SSM3-VH	VH1	2	CARGTVVGRSGYYYGMDVWG
SSM4-VH	VH5	2	CARRAPPLSGWYYRALDCWG
SSM5-VH*	VH3	3	CARDRSSSLSYSWYFDLWG
SSM6-VH	VH3	4	CTRGVNYEGFRLDDWG
SSM7-VH	VH5	1	CARTQWEVINPYYSDFWG
JMB1-VH†	VH1	1	CARDRGGGDLYHWG
JMB2-VH*	VH1	2	CARVQWLNALDFWG
JMB3-VH*	VH3	5	CARYHDKLLGVIPYWG

Table 5a. CDR3 regions of clonally expanded IgG-VH reconstructed sequences

Name of the rebuilt light chain clones	Corresponding Ig-VL family	Matching Ig-VL seq. obtained	Amino acids sequence of CDR3 region of corresponding Ig-VL clones
GKD1-kC	Vk1	6	CQQSYSIPPTFG
GKD2-kC	Vk3	3	CQQRANWPPITFG
GKD3-kC*	Vk1	5	CQESYSTLVTFG
GKD4-kC*	Vk3	4	CQHYGYSPVTFG
GKD5-kC*	Vk2	2	CMQRLEFPPTFG
GKD6-kC	Vk1	4	CQQNYNTRTFG
GKD7-λC	Vλ3	5	CNSRDSSGNHWVFG
SSM1-Vλ	Vλ3	3	CQAWDSTTVVFG
SSM2-Vλ	Vλ3	2	CQVWDSSTVVFG
SSM3-Vλ	Vλ3	4	CQAWDSSTVLFG
SSM4-Vλ	Vλ3	3	CQSSDSSGTYGIFG
SSM5-Vλ*	Vλ3	4	CQVWDTSSDHVVFG
SSM6-Vk	Vk2	2	CLQALQTPLTFG
SSM7-Vk	Vk4	2	CQQYYNTPHTFG
JMB1-Vk†	Vk4	1	CQQYDNLPPYTFG
JMB2-Vk*	Vk4	2	CLQYYTDPYTFG
JMB3-Vk*	Vk4	2	CQQYRRLPQISFG

Table 5b. CDR3 regions of clonally expanded Ig-light chain reconstructed sequences

Clonally expanded sequences reproduced in recombinant antibody form recognized respective antigen targets *in vitro.
† A single plasma cell/plasmablast sequence (not clonally expanded) reproduced in recombinant form.

Analysis of clonally expanded plasma cells/plasmablasts (cePc)

Sequences sharing more than 95% nucleotide identity, having similar or identical CDR3 regions and belonging to the same V(D)J germline family were considered clonally expanded. Alignment of Ig-heavy chain variable region genes in groups of identical sequences yielded information on a total of 57 independent cePc clones. Seven cePc clones belonged to the CSF plasma cells/plasmablasts of GKD, another seven cePc to SSM, two cePc clones to JMB, 21 cePc to KKM and 20 cePc clones to BRM (**Table 4a**, Pg.40). Out of 57 identified heavy chain cePc clones, 38 were expressed with matching Ig-Vκ cePc (66.6%) and 19 with Ig-Vλ cePc (33.3%) clones. Eight more cePc clones belonging to kappa light chains and two more cePc clones belonging to the lambda light chains were identified. However their matching IgG heavy chain sequences could not be discovered.

From a total of 508 CSF IgG-VH sequences obtained, 180 sequences (35.4%) belonged to the 57 cePc clone populations and remaining 328 were unique single sequences. The number of cePc sequences belonging to each cePc clones was highly variable. Repertoire analysis of the IgG heavy chain cePc sequences from each patient revealed, 31 of 86 heavy chain sequences (36.0%) from GKD, 17 of 37 (45.9%) from SSM, 7 of 42 (16.6%) from JMB, 57 of 161 (35.4%) from KKM, and 68 of 182 sequences (37.3%) from BRM were belonged to cePc clone populations (**Table 4a**, Pg.40).

The cumulative cePc sequences from five patients revealed that most IgG-VH cePc sequences represented V_H1 family (13.1%), followed by V_H3 (12.7%), V_H4 (8.0%), V_H5 (0.9%) and V_H7 (0.3%) families (**Table 4b**, Pg.40). Out of 305 Ig-Vκ sequences obtained, 118 sequences (38.6%) were identified in the cePc clone populations. Similarly, from 114 CSF Ig-Vλ sequences obtained, 65 sequences (57.0%) were identified in cePc clones populations.

The 118 Igκ cePc sequences belonged to a total of 46 cePc individual clones and mostly represented the $V_κ1$ family (19.3%), followed by $V_κ3$ (15.4%), $V_κ2$ (1.9%) and $V_κ4$ (1.9%) families. We did not find any Igκ cePc sequence representing $V_κ5$ family. The 65 lambda chain cePc sequences belonged to a total of 21 unique cePc clones and mostly represented the $V_λ3$ family (32.4%), followed by $V_λ2$ (16.6%), $V_λ1$ (4.3%), $V_λ6$ (1.7%), and $V_λ8$ (1.7%) families (**Table 4b**, Pg.40).

Name of the rebuilt IgG-VH clones	Corresponding V(D)J germline combination	Number of amino acid mutations in corresponding IgG-VH clones.						
		FR1	CDR1	FR2	CDR2	FR3	CDR3	Total mutations
GKD1-VH	VH3(D6)JH6	2	1	-	1	5	-	9
GKD2-VH	VH3(D6)JH4	-	2	-	1	-	-	3
GKD3-VH*	VH1(D1)JH6	1	3	1	1	3	-	9
GKD4-VH*	VH4(D3)JH6	1	1	2	2	-	-	6
GKD5-VH*	VH4(D1)JH3	2	2	-	-	3	-	7
GKD6-VH	VH4(D3)JH4	2	1	-	1	6	-	10
GKD7-VH	VH1(D3)JH6	1	4	2	3	3	-	13
SSM1-VH	VH3(D3)JH6	1	1	1	1	4	-	8
SSM2-VH	VH4(D5)JH2	-	1	1	1	4	-	7
SSM3-VH	VH1(D6)JH6	-	-	-	4	4	-	8
SSM4-VH	VH5(D6)JH5	3	3	1	2	4	-	13
SSM5-VH*	VH3(D6)JH2	1	-	-	-	-	-	1
SSM6-VH	VH3(D3)JH4	1	1	2	1	9	1	15
SSM7-VH	VH5(D1)JH4	-	3	2	1	-	-	6
JMB1-VH†	VH1(D2)JH4	-	4	5	3	5	-	17
JMB2-VH*	VH1(D6)JH3	1	1	1	1	4	-	8
JMB3-VH*	VH3(D2)JH5	3	1	3	3	10	1	21

Table 6a. Number of amino acid mutations in the reconstructed clonally expanded IgG- heavy chain variable regions from corresponding V(D)J germline genes.

Name of the rebuilt Ig-VL clones	Corresponding V(D)J germline combination	Number of amino acid mutations in corresponding Ig-VL clones.						
		FR1	CDR1	FR2	CDR2	FR3	CDR3	Total mutations
GKD1-kC	Vk1(-)Jk4	2	3	-	-	2	1	8
GKD2-kC	Vk3(-)Jk5	-	1	-	-	-	1	2
GKD3-kC*	Vk1(-)Jk5	-	1	2	-	3	1	7
GKD4-kC*	Vk3(-)Jk4	-	3	3	-	1	2	9
GKD5-kC*	Vk2(-)Jk4	1	-	-		3	1	5
GKD6-kC	Vk1(-)Jk1	-	2	2	1	1	2	8
GKD7-λC	Vλ3(-)Jλ3	3	-	2	-	3	-	8
SSM1-Vλ	Vλ3(-)Jλ2	-	-	-	1	-	-	1
SSM2-Vλ	Vλ3(-)Jλ2	-	-	-	1	-	-	1
SSM3-Vλ	Vλ3(-)Jλ2	-	-	-	1	-	-	1
SSM4-Vλ	Vλ3(-)Jλ1	1	1	1	1	-	1	5
SSM5-Vλ*	Vλ3(-)Jλ2	-	-	-	-	-	1	1
SSM6-Vk	Vk2(-)Jk4	1	3	1	1	1	1	8
SSM7-Vk	Vk4(-)Jk2	1	4	-	-	1	1	7
JMB1-Vk†	Vk1(-)Jk2	2	-	-	-	-	-	2
JMB2-Vk*	Vk1(-)Jk2	2	1	4	1	2	3	13
JMB3-Vk*	Vk1(-)Jk3	5	2	4	-	9	2	22

Table 6b. Number of amino acid mutations in the reconstructed clonally expanded Ig- light chain variable regions from corresponding V(D)J germline genes.

Clonally expanded sequences reproduced in recombinant antibody form recognized respective antigen targets *in vitro.
† A single plasma cell/plasmablast sequence (not clonally expanded) reproduced in recombinant form.

Cloning of recombinant human monoclonal antibodies (rhuMAb)

Clonally expanded, paired Ig-heavy and light chain variable region sequences were selected for recombinant monoclonal antibody production; either by synthesizing the sequences and sub-cloning, or by 2^{nd} round PCR with primers containing restriction sites and directly cloning into the respective mammalian expression vectors (**Fig. 11**, Pg.39). The Ig-variable regions were cloned in frame with the respective human Igγ1, Igκ or Igλ2 constant region genes encoded by the mammalian expression vectors (**Fig. 8**, Pg.28). All cloned expression vectors were sequenced to confirm the presence of Ig-V region inserts with 100% identity to the respective original PCR products.

We have so far successfully generated 17 functional recombinant human monoclonal antibodies from CSF-derived cePc of three patients among five with AIE. Seven rhuMAb (SSM1-7) were reconstructed from a patient pre-diagnosed with anti-NMDA receptor encephalitis. Another seven antibodies (GKD1-7) were regenerated from a patient pre-diagnosed with anti-LGI1 encephalitis and two rhuMAb (JMB 2 & 3) were rebuilt from CSF-cePc clones of a patient pre-diagnosed with anti-GAD_{65} encephalitis. A rhuMAb, named JMB1 was reproduced from a unique single plasma cell/plasmablast that was not clonally expanded in the CSF of the patient with anti-GAD_{65} autoantibody.

Amino acid sequence of the CDR3 region was used as a unique identifier of clonal populations and the nucleic acid sequence of the Ig-V regions were used to identify the closest germline family. Number of clonally expanded Ig-sequences belonging to each reconstructed cePc, varies from 2 to 6 (**Table 5a&b**, Pg.44). Most of the cePc sequences from CSF of each patient were strongly hypermutated containing silent and replacement mutations indicating an ongoing antigen driven humoral immune response in the CSF compartment (**Table 6a&b**, Pg.46).

Production of rhuMAb

Polyethylenimine (PEI) mediated co-transfections of Ig-HC and matching Ig-LC expression vectors into FreeStyle 293-F cells were carried out to produce recombinant monoclonal antibodies *in vitro*. Up to 95% transfection efficiency was observed using PEI for an eGFP control plasmid. The secreted rhuMAb were purified from the supernatant of transfected cells using either protein G HP columns or Magne protein G beads, as described in materials and methods. Around 90% of individual transfections produced functional rhuMAb at concentrations from 30µg/ml to 140µg/ml with an average concentration of 80µg/ml from 200 ml of supernatant. Complete functional antibody productions were confirmed by SDS gel electrophoresis (**Fig. 14**).

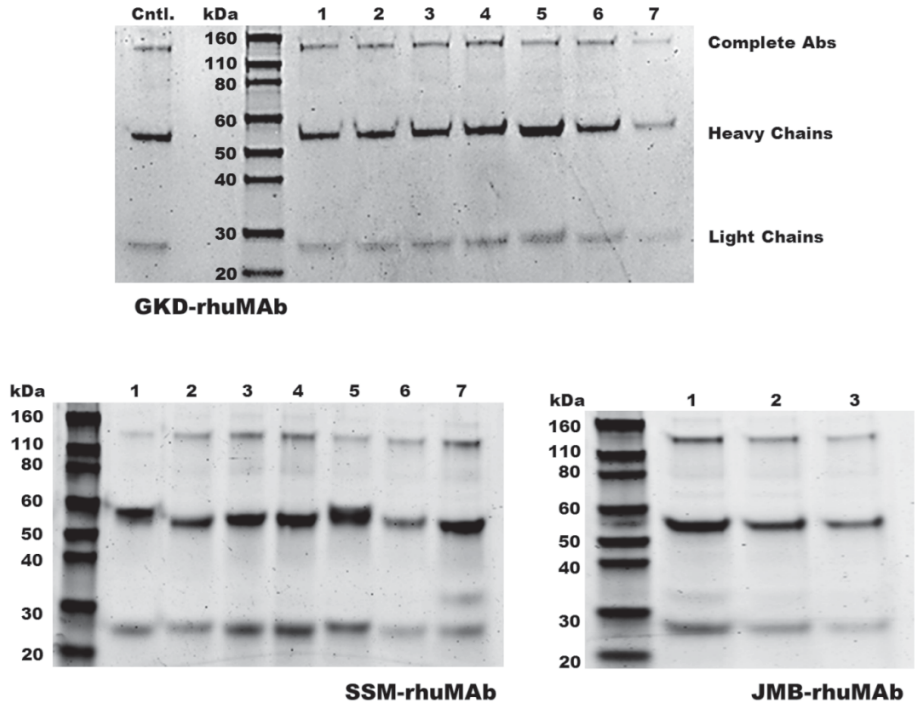

Figure: 14. SDS-gel pictures of purified recombinant human monoclonal antibodies (rhuMAb). Samples were mixed with NuPAGE reducing agent at 60°C for 10 min. Around 5 µg of each rhuMAb was run on 4-16 % Precise Protein gel. The antibody bands were visualized with Gel-code Blue stain reagent. The numbers on each lane represents an antibody name, for example; lane 3 of GKD-rhuMAb gel represents GKD3 antibody. Novex sharp pre-stained protein standard, and a control antibody purified in similar conditions as rhuMAb were also loaded.

Characterization of rhuMAb

All purified rhuMAb were sent to EUROIMMUN AG, Luebeck-Germany for initial characterization. The reactivities of all the ruhMAb against prediagnosed target antigens of the respective patient were investigated. Some of the patient-derived recombinant antibodies recognized their antigen specificity *in vitro*. Out of 17 rhuMAb reconstructed, six antibodies GKD3, GKD4, GKD5, SSM5, JMB2 and JMB3 showed a clear reactivity to their respective target antigens. Three GKD rhuMAb, namely GKD3, GKD4 and GKD5 strongly reacted to LGI1 protein. Among seven SSM rhuMAb, only SSM5 reacted to the NR1 subunit of NMDA receptor. Two of the JMB rhuMAb, namely JMB2 and JMB3 showed high affinity for GAD_{65} auto-antigen, whereas all the remaining rhuMAb did not show any binding to the EUROIMMUN neuronal antigen panel *in vitro*.

To reconfirm rhuMAb reactivity profile to the known antigens, we re-characterized all the rhuMAb in our laboratory by immunocytochemistry (ICC) and immunoprecipitation (IP) experiments.

Immunocytochemistry

All the rhuMAb were tested in immunocytochemistry on HEK-293 cells transfected with mammalian expression vectors expressing cDNA of respective antigen targets such as human LGI1, human GAD_{65}, rat NR1 subunit and rat NR1/NR2B heteromers. Our immunostaining results for rhuMAb were in accordance with the findings of EUROIMMUN AG.[117]

HEK-293 cells expressing human LGI1 secreted protein were pre-incubated with Brefeldin-A (an inhibitor of protein secretion[38]) before immunostaining with GKD1-7 rhuMAb. The GKD3, GKD4 and GKD5 rhuMAb recognized the human LGI1 protein in the cytoplasm without uniform distribution on the cell surface (**Fig. 15**, Pg.50). None of the GKD1-7 rhuMAb antibodies reacted when tested on the non-transfected HEK-293 cells.

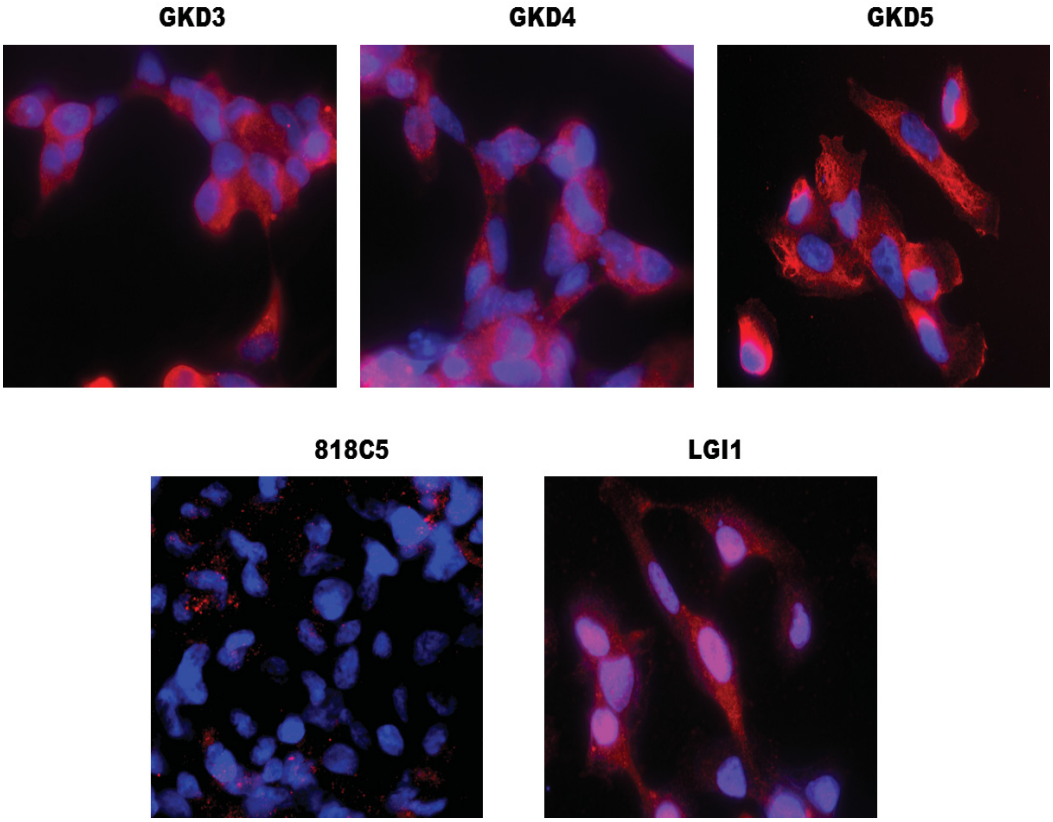

Figure: 15. Immunocytochemistry of HEK-293 cells expressing the human LGI1 protein.
The HEK-293 cells transfected with LGI1 (a neuronally secreted protein) were incubated with 100ng/ml Brefeldin-A (an inhibitor of protein secretion[38]) for one hour before fixed, permeabilized, immunostained with GKD1-7 rhuMAb and detected with Cy3 labeled secondary antibodies. Nuclei were stained with DAPI. The GKD3, GKD4 and GKD5 strongly reacted to human LGI1 protein in the cytoplasm of the transfected cells. A commercially available rabbit polyclonal anti-LGI1 antibody was used as positive control. Chimeric 818C5, an anti-MOG Ab, was included as a negative control. Images were acquired with 60 x oil-immersion objective.

Among SSM1-7 rhuMAb, SSM5 clearly reacted with the rat NR1 subunit of NMDA receptor on HEK-293 cells transfected with NR1 subunit alone. The binding pattern of SSM5 to HEK-293 cells expressing NR1 subunit alone was similar to the commercial anti-NR1 antibody (**Fig. 16A**, Pg.51).

Double transfected HEK-293 cells with rat NR1/NR2B heteromers were immunostained with SSM5 and a commercial rabbit anti-NR2B subunit antibody. The reactivity of SSM5 and an anti-NR2B Ab were clearly co-localized on the cells expressing NR1/NR2B heteromers, whereas cells expressing only NR1 subunits were stained with only SSM5 rhuMAb (**Fig. 16B**). The SSM5 rhuMAb did not react when tested on the non-transfected HEK-293 cells.

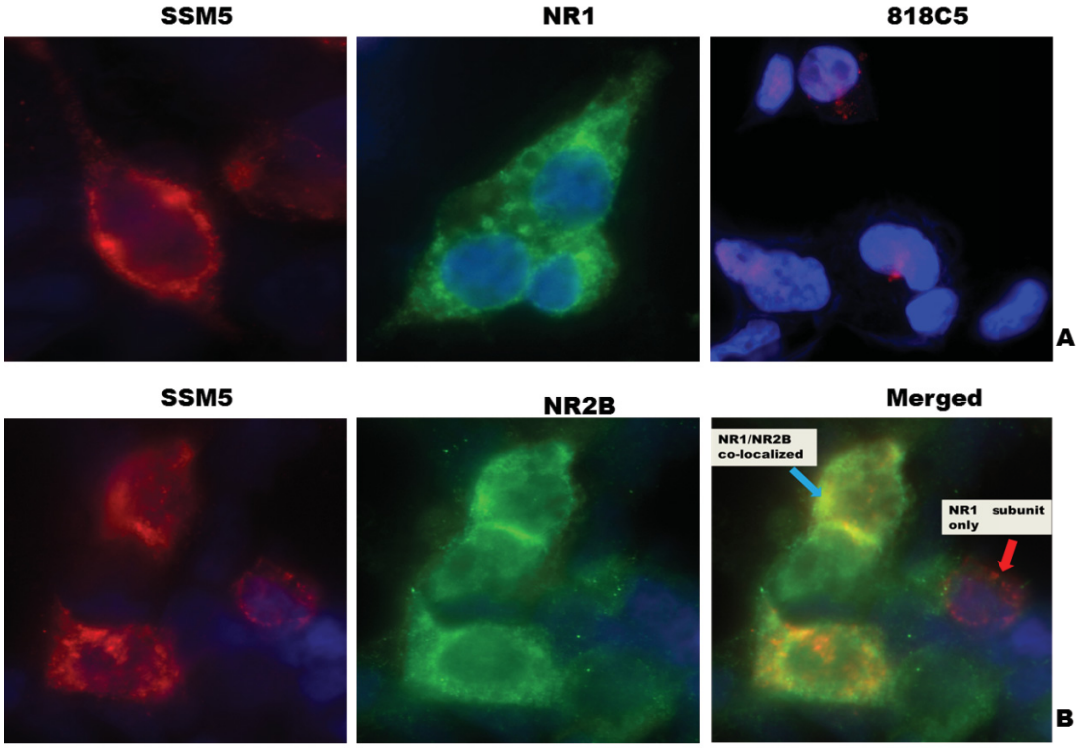

Figure: 16. Immunocytochemistry of cells expressing NR1 subunit alone (A) and NR1/NR2B heteromers (B) of the NMDA receptor. HEK-293 cells transfected with rat NR1/NR2B heteromers (functional receptors) were cultured for three days in the presence of 500 µM ketamine (an inhibitor of NMDA receptor), fixed, immunostained with SSM1-7 rhuMAb and detected with Cy3 labeled secondary antibody. Commercially available rabbit anti-NR1 and anti-NR2B antibodies were used as positive controls and detected with Alexa-488 labeled secondary antibody. Nuclei were stained with DAPI. SSM5 reacted with NR1 subunit alone in a similar pattern as control NR1 antibody (**A**). Figure **B** shows co-localization of NR1&NR2B subunits stained with SSM5 and a control NR2B antibody on transfected cells. Chimeric 818C5, an anti-MOG Ab, was included as a negative control. Images were acquired with 60 x oil-immersion objective.

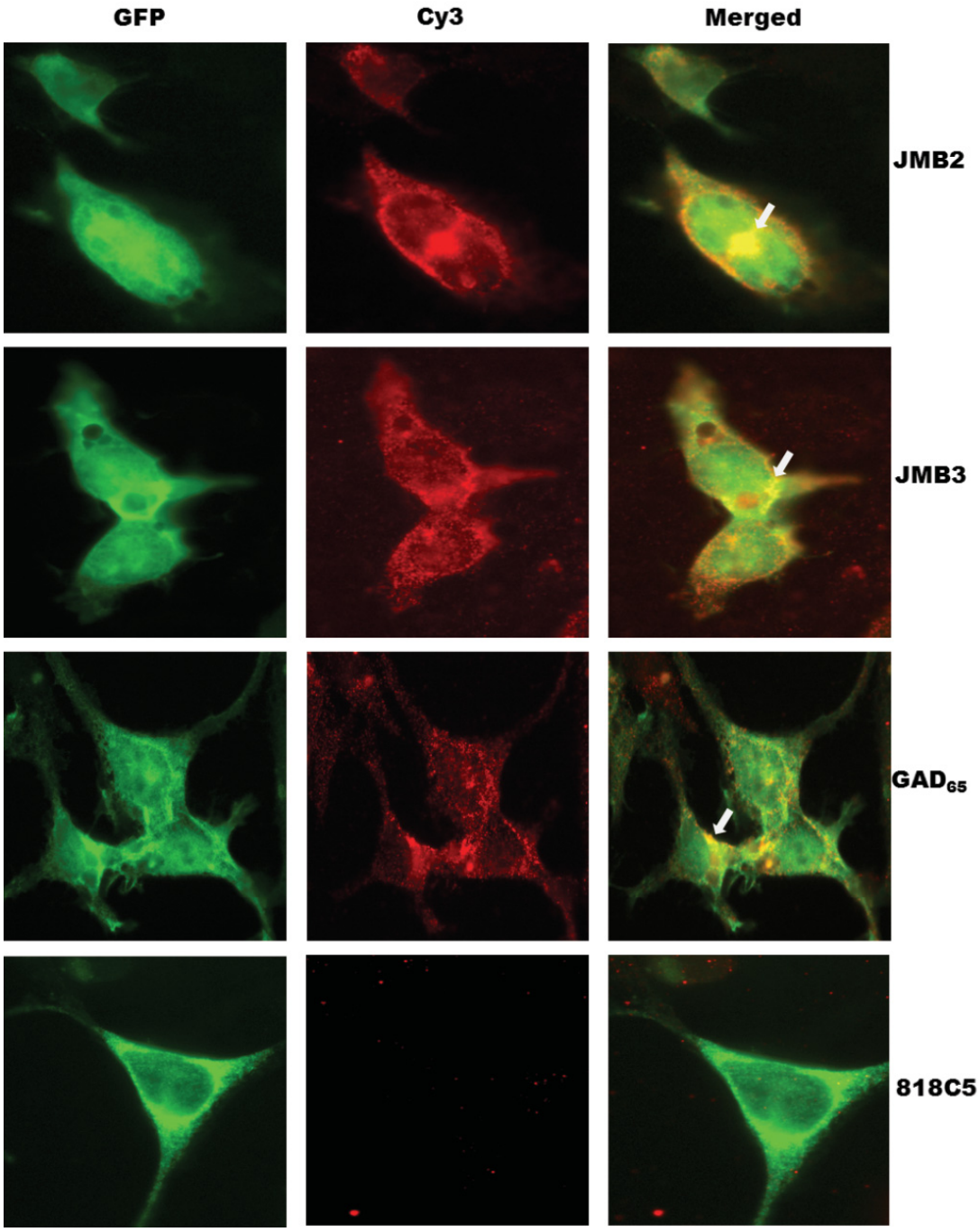

Figure: 17. Immunocytochemistry of cells expressing the human GAD_{65} protein.
HEK-293 cells transfected with a eukaryotic expression vector co-expressing human GAD_{65} and EmGFP (cytosolic) were fixed, permeabilized, immunostained with JMB rhuMAb and detected with Cy3-labeled secondary antibodies. JMB2 and JMB3 reacted to human GAD_{65} protein and also co-localized with GFP in the membrane terminal of the transfected cells (**Arrow**). A commercial anti-GAD_{65} antibody was included as a positive control. Chimeric 818C5, an anti-MOG Ab, was included as a negative control. Images were acquired with 60 x oil-immersion objective.

The reactivity profile of JMB1-3 rhuMAb to GAD_{65} enzyme was determined on HEK-293 cells transfected with a eukaryotic expression vector co-expressing human GAD_{65} and EmGFP. The JMB2 and JMB3 rhuMAb reacted with human GAD_{65} and co-localized with GFP in the membrane terminal of the transfected cells, confirming the human GAD_{65} as a target antigen (**Fig. 17**, Pg.52). The JMB rhuMAb did not react when tested on the non-transfected HEK-293 cells.

JMB1 rhuMAb reproduced from a non-clonal CSF plasma cell/plasmablast did not show any reactivity to GAD_{65}. An antibody specific to an irrelevant antigen was used as a negative control in every ICC and IP experiment.

Immunoprecipitation

It was previously shown that synaptic autoantigens can be isolated by use of immunoprecipitations (IPs) with antibodies obtained from sera or CSF of AIE patients.[38] Likewise, IPs using rhuMAb were performed to identify antigenic targets from rat, marmoset and human brain tissues. Commercially available antibodies to the respective target antigens were used as positive controls. Precipitated proteins were visualized on silver stained gels and confirmed by western blot detection with commercial antibody specific for the antigen tested, such as LGI1, NR1, and GAD_{65}.

LGI1 was identified as the target antigen by IPs using GKD3 rhuMAb on silver stained gels and also by Western blots. A distinct visible band of around 70 kDa corresponding to the LGI1 protein was detected in the membrane fractions of rat, marmoset and human brains (**Fig. 18A-D**, Pg.54). At high concentrations, GKD1 and GKD7 showed very weak binding to LGI1 in IPs (data not shown). No reactivity to any other antigens was found using the GKD rhuMAb.

Similarly, NR1 subunit of NMDA receptor was identified as the target antigen by IP using SSM5 rhuMAb. A band of around 120 kDa corresponding to NR1 subunit was detected by Western blot from tissue membrane fractions of marmoset and human brains (**Fig. 18E&F**, Pg.54). None of the other rhuMAb recognized any antigen tested in the membrane fractions of rat, marmoset and human brains.

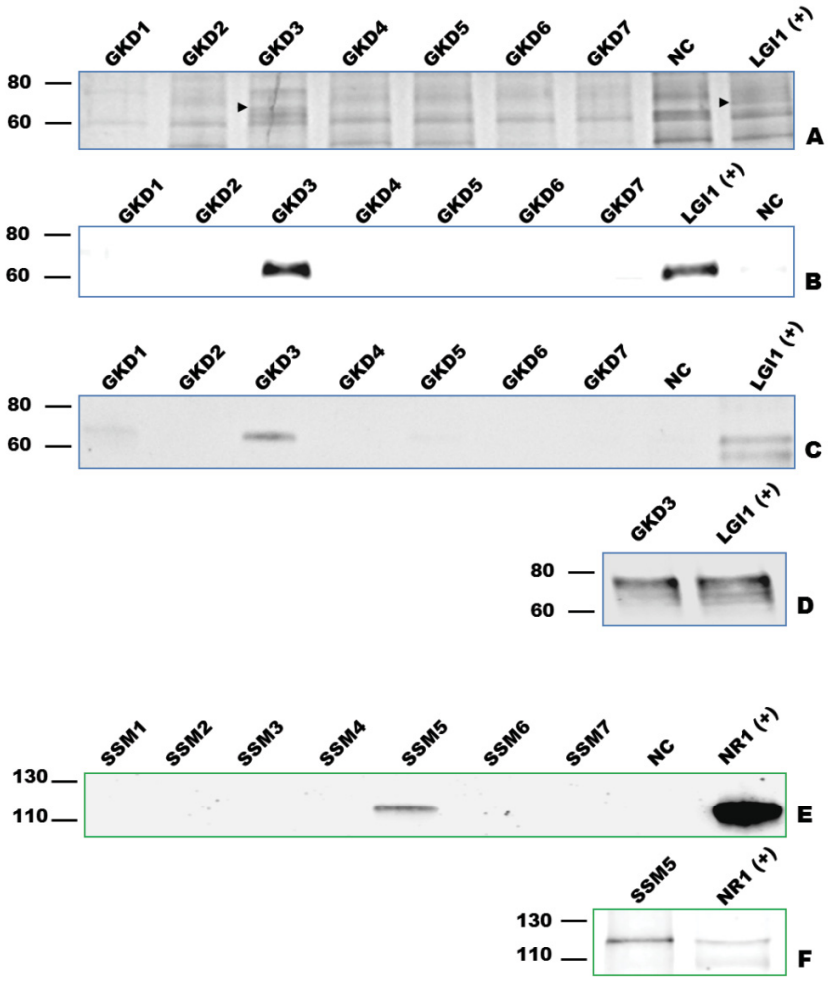

Figure: 18. Immunoprecipitations using recombinant human monoclonal antibodies (rhuMAb).

Precipitated proteins were visualized on a silver stained gel (**A**) and confirmed by Western blot detection with commercial antibodies (**B-F**). A band of around 70 kDa corresponding to LGI1 protein was detected using GKD3, in the membrane fractions of rat (**A&B**), marmoset (**C**) and human (**D**) brains. A band of around 120 kDa corresponding to the NR1 subunit of NMDA receptor was identified using SSM5 in the membrane fractions of marmoset (**E**) and human (**F**) brains. Commercially available antibodies to the respective target antigen were used as positive control in IPs and in western blot detections. An antibody 12D7 specific for an irrelevant target NY-ESO-1, was included as a negative control (**NC**) for IP experiments.

DISCUSSION

The autoimmune encephalitis (AIE) syndromes associated with autoantibodies against neuronal cell-surface or synaptic proteins belong to a new category of diseases that has changed paradigms in the diagnosis and treatment of disorders that were previously mischaracterized or unknown. The pathogenic properties of antineuronal antibodies have been characterized in a small number of studies, which support their pathogenic role in the underlying neurological disease. The cognate targets of some of these autoantibodies have been identified, e.g. NMDA receptor, AMPA receptor, leucine-rich glioma inactivated protein 1 (LGI1), contactin-associated protein-like 2 (CASPR2), glutamic acid decarboxylase (GAD_{65}) and others.

Affected patients often display a variety of "psychiatric" symptoms such as behavioural changes, anxiety or psychosis followed by seizures, decline of consciousness, aphasia, and abnormal movements. Studies of AIE have revealed that it can occur with or without an underlying tumor, affects patients of all ages,[118] and has exposed novel mechanisms of how autoantibodies might alter memory, behavior, psychosis, seizures and abnormal movements.[119] Most commonly AIE is associated with ovarian teratoma or tumors in thymus, lung or breast.

Studies have shown that the associated autoantibodies mediate neuronal dysfunction by direct interaction with the target antigens. It has been postulated that although some of these antigens are intracellular, they can be exposed on the cell surface during synaptic vesicle recycling, and there is evidence that both B- and T-cell mechanisms underlie the neuronal pathology.[121, 122] In cancer-associated disorders, the immune response is likely initiated against neuronal antigens expressed by the tumor, but what is the immunological trigger in non-tumor associated autoimmune encephalitis is not yet understood. The occurrence of a viral-like prodrome in many patients suggests that infections with viruses such as herpes simplex virus 1 potentially play a role in activating the autoimmune response against neuronal proteins like the NMDA receptor.[61]

The source of origin of autoantibodies in patients with AIE is not yet understood; it is not clear whether the autoantibodies are generated intrathecally or produced in periphery system and enter into the CNS via crossing the blood brain barrier or vice versa.

Previous studies on autoantibodies isolated from cerebrospinal fluid (CSF) and serum of patients with AIE have described the presence of several anti-neuronal autoantibodies.[5, 38] Since the autoantibodies and oligoclonal bands (OCB) are products of clonally expanded plasma cells/plasmablasts (cePc) in the CSF of patients with different kind of autoimmune disorders, such as multiple sclerosis,[108, 109] we presumed that the autoantibodies in the CSF of patients with AIE are also the products of CSF-derived cePc.

The present study was intended to analyze the CSF $CD138^+$ plasma cell/plasmablast repertoire of patients with AIE and to re-construct some of the anti-neuronal autoantibodies produced by them in the form of recombinant human monoclonal antibodies (rhuMAb), as described elsewhere for multiple sclerosis.[109, 113]

Single CSF $CD138^+$ plasma cell and $CD138^+/CD19^+$ plasmablast were isolated from five AIE patients, by FACS. To identify CSF cePc and characterize the Ig-gene family usage in the plasma cells/plasmablasts, we first performed single-cell RT-PCR of rearranged IgG-VH, Ig-Vκ and Ig-Vλ genes. Alignment of IgG-heavy chain variable region genes in groups of identical sequences yielded information on 57 independent cePc clones from the CSF of five AIE subjects. All the Ig-heavy and light chain variable region sequences of cePc contained mutations, supporting ongoing antigen-driven maturation of immune responses in the CSF of affected patients. A heterogeneous usage of IgG-VH, Ig-Vκ and Ig-Vλ gene families were identified in the CSF plasma cells/plasmablasts.

Investigation of Ig-gene repertoire could be useful to understand the selection of the germline gene family in the maturation process of the CSF plasma cells/plasmablasts of patients with AIE. In this study, we have analyzed five patients pre-diagnosed with different kind of anti-neuronal autoantibodies. As characterized by an online database (http://www.ncbi.nlm.nih.gov/igblast/), the Ig-gene repertoire of individual patients with unique autoantibodies showed different patterns. A patient pre-diagnosed with anti-LGI1 autoantibodies (GKD) had a clear overrepresentation of V_H4 family. The V_H1 family was underrepresented in a patient with anti-NMDA receptor autoantibodies (SSM). Two patients with anti-CASPR2 autoantibodies (KKM & BRM) had similar patterns of germline gene families representation in order of $V_H3>V_H1>V_H4>V_H5$. However, one of the patients with anti-CASPR2 autoantibodies also represented V_H7 family. The V_H1 family was mostly

represented in a patient pre-diagnosed with anti-GAD_{65} (JMB) autoantibody (**Table 3a,** Pg.38). Further studies on the CSF plasma cells/plasmablasts from a larger number of samples/patients prediagnosed with similar anti-neuronal autoantibodies (e.g. anti-NMDA receptor Ab) could give more detailed information about the representation of Ig-gene families and source of origin for the self-reactive anti-neuronal antibodies.

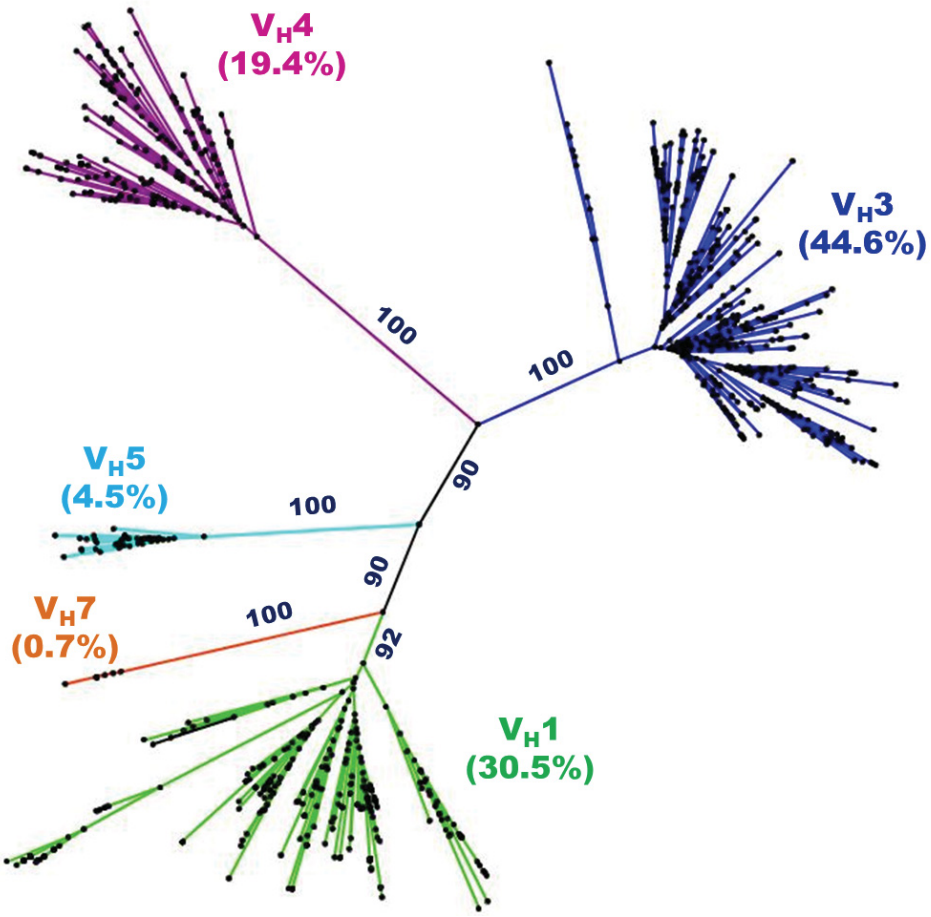

Figure: 19. Unrooted phylogenetic tree of cumulative IgG-VH sequences derived from the CSF plasma cells/plasmablasts of five AIE patients.

The tree representing IgG-VH gene family repertoire calculated from 508 sequences. The branch length and distance between sequences correspond to sequence similarity/dissimilarity, shorter and closer branches relate to a greater sequence similarity. Sequences belonging to one family share similarities and group together. Thus, each colored branch of the tree represents a single VH family. The external node of a branch represents a 'leaf' or a 'sequence'. For the clarity of the picture, 'sequences' or 'leaves' on the external nodes are not shown. The bootstrap support values for each branch on the tree were calculated based on 100 resamplings of the original data set.

Even though all the five patients diagnosed with different kind of anti-neuronal autoantibodies, they are usually presented with similar kind of symptoms, receive mostly similar therapy and characterized under a same group of disease called 'autoimmune encephalitis'. Therefore, we also analyzed the cumulative Ig-gene repertoire of CSF plasma cells/plasmablasts of all the five patients, to investigate a common pattern of Ig-gene representations in AIE.

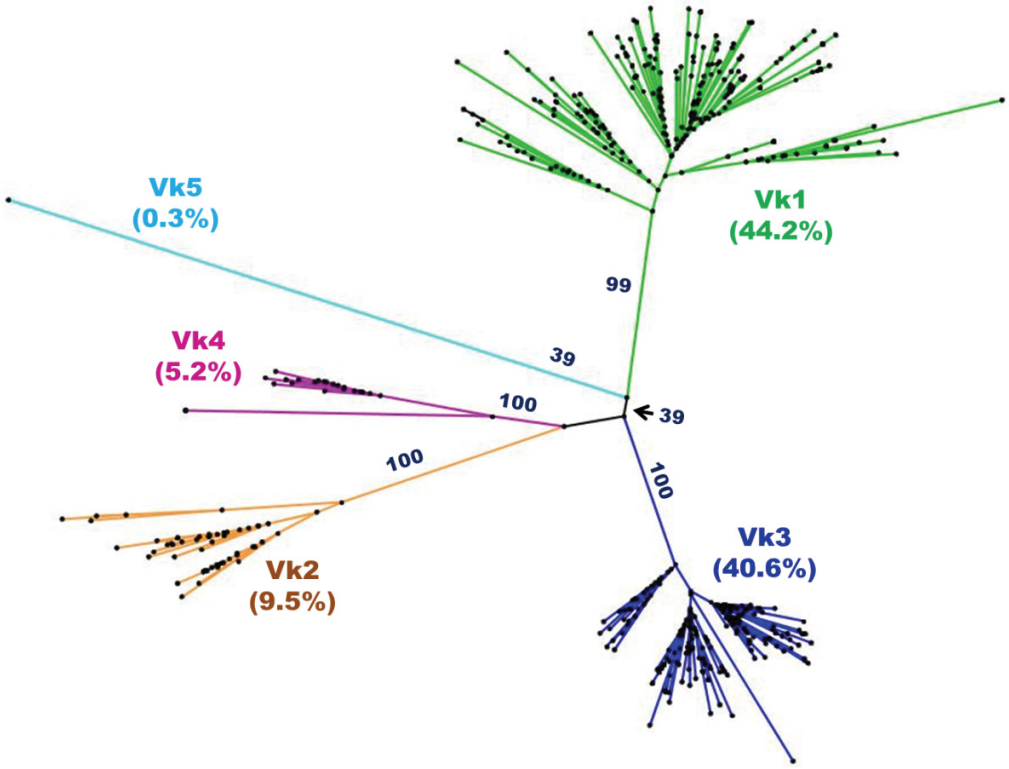

Figure: 20. Unrooted phylogenetic tree of cumulative Ig-Vκ sequences derived from the CSF plasma cells/plasmablasts of five AIE patients.

The tree representing Ig-Vκ gene family repertoire calculated from 305 sequences. Each colored branch of the tree represents a single Vκ family and each external node of a branch represents a 'leaf' or a 'sequence'. The bootstrap support values for each branch were calculated based on 100 resamplings of the original data set.

Cumulative repertoire analysis revealed IgG-VH sequences were derived from five germline segments in order of $V_H3>V_H1>V_H4>V_H5>V_H7$ (**Fig. 19**, Pg.57). The Ig-Vκ sequences were also derived from five germline segments in the order of $V_κ1>V_κ3>V_κ2>V_κ4>V_κ5$ (**Table 3b**, Pg.38 and **Fig. 20**, Pg.58), whereas Ig-Vλ sequences were most heterogeneous as they were derived from seven germline gene segments in order of $V_λ3>V_λ2>V_λ1>V_λ6>V_λ7=V_λ8>V_λ9$ (**Table 3b**, Pg.38 and **Fig. 21**, Pg.59). Clonally expanded sequences were found in all represented heavy chain families mentioned above. However, no cePc sequences were found representing the light chain families $V_κ5$, $V_λ7$ and $V_λ9$.

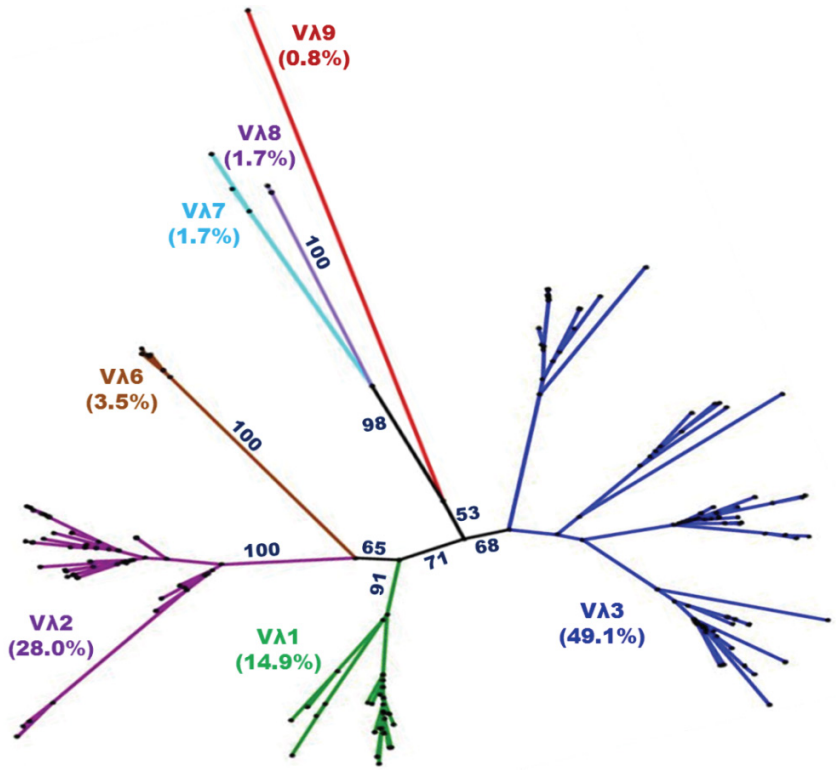

Figure: 21. Unrooted phylogenetic tree of cumulative Ig-Vλ sequences derived from the CSF plasma cells/plasmablasts of five AIE patients.

The tree representing Ig-Vλ gene family repertoire calculated from 114 sequences. Each colored branch of the tree represents a single Vλ family and each external node of a branch represents a 'leaf' or a 'sequence'. The bootstrap support values for each branch were calculated based on 100 resamplings of the original data set.

Investigation of CSF plasma cells/plasmablasts repertoire of AIE patients could also be useful to understand the generation of cePc clone population and Ig-genes producing self-reactive autoantibodies. In this study, we have so far successfully generated a set of 17 recombinant human monoclonal antibodies (rhuMAb) from CSF-cePc from three of five patients with AIE. From these 17, seven antibodies were regenerated from a patient prediagnosed with anti-NMDA receptor encephalitis (SSM1-7). Another seven rhuMAb antibodies were reconstructed from a patient pre-diagnosed with anti-LGI1 encephalitis (GKD1-7), and three rhuMAb were rebuilt from a patient pre-diagnosed with anti-GAD_{65} encephalitis (JMB1-3). Among JMB1-3 rhuMAb, only JMB2 and JMB3 were rebuilt from CSF-cePc clones, whereas the JMB1 rhuMAb was reproduced from a unique single plasma cell/plasmablast that was not detectably clonally expanded in the CSF of the patient with anti-GAD_{65} antibody. RhuMAb from cePc of two patients prediagnosed with anti-CASPR2 autoantibodies are currently in different stages of cloning and recombinant expression.

While our initial approach on characterization of the reconstructed rhuMAb mainly focused to investigate, whether clonally expanded CSF plasma cells indeed produce the antibodies specific for the target antigens prediagnosed in the respective patient, cePc derived recombinant antibodies could also be used to identify novel target antigens in AIE patients with unkown antibody signatures. The reactivity profiles of rhuMAb are summarized in the **table 7** (Pg. 61).

Out of 17 rhuMAb reconstructed six antibodies, namely GKD3, GKD4, GKD5, SSM5, JMB2 and JMB3 showed a clear reactivity to their presumed target antigens *in vitro*. GKD1 and GKD7 additionally showed very weak binding to LGI1 in IPs (data not shown), and all the other antibodies did not show any reactivity to the antigens tested. Interestingly, the antigen recognition patterns of rhuMAb rebuilt from different groups of cePc of the same patient do not necessarily match: for instance - GKD3, GKD4 and GKD5 strongly reacted to human LGI1 in immunocytochemistry (ICC). However, only GKD3 could recognize LGI1 in IP experiments using membrane fractions from human, marmoset and rat brains. Similarly, JMB2 and JMB3 only reacted to human GAD_{65} in ICC but not in IPs. On the other hand, SSM5 showed a clear reactivity to the NR1 subunit of NMDA receptor both in ICC and IP.

The SSM5 rhuMAb strongly reacted with NR1 subunit in IP experiments using membrane fractions of human and marmoset brains. Surprisingly, the SSM5 rhuMAb clearly reacted with rat NR1 subunit in transfected HEK-293 cells, but did not react in IP using membrane fractions of rat brain. The rational for not recognizing rat brain NR1 subunit in IP could be associated with the SSM5 reactivity with primate cell specific posttranslational modifications of NR1 subunit. However, we do not have any additional evidence to support this hypothesis.

	Immunocytochemistry (using transfected HEK-293 cells)		Immunoprecipitation (using brain tissue fractions)			Antigens
rhuMAb	Rat protein	Human protein	Rat	Marmoset	Human	
GKD3	Nt.	✓	✓	✓	✓	LGI1
GKD4	Nt.	✓	×	×	×	LGI1
GKD5	Nt.	✓	×	×	×	LGI1
SSM5	✓	Nt.	×	✓	✓	NR1
JMB1	Nt.	×	×	×	×	
JMB2	Nt.	✓	×	×	×	GAD_{65}
JMB3	Nt.	✓	×	×	×	GAD_{65}

Table 7. The reactivity profile of rhuMAb

Not tested = (Nt.) **Not reacted (×)** **Reacted (✓)**

The reason why the antigen specificity of GKD4, GKD5, JMB2 and JMB3 rhuMAb could only be revealed by ICC has remained undetermined. However, it is possible that the epitopes recognized by these autoantibodies may depend on their intact conformation within the cell membrane and/or posttranslational modifications.

We were also interested to investigate if a unique single plasma cell/plasmablast, which is not clonally expanded in the CSF of patients with AIE, could also produce self-reactive antibodies. The JMB1 rhuMAb reproduced from a non-cePc did not show any reactivity to the human GAD_{65} auto-antigen in the initial characterizations. However, further characterizations of JMB1 rhuMAb for other self-antigens in patients with AIE have to be determined. The presence of autoantibodies targeting two or more self-antigens in patients with AIE has been reported previously.[96, 20] We presume a diversity of potential other

antigen targets for our CSF cePc derived remaining 10 rhuMAb, which did not react to the antigens tested in initial characterization. Further experimental effort is being made to identify the exact target antigens of patient-derived remaining rhuMAb.

In conclusion, our findings provide evidence that clonally expanded intrathecal plasma cells/blasts contribute to the production of antineuronal autoantibodies in AIE patients. By reconstructing functional autoantibodies from CSF cePc in the form of rhuMAb, we demonstrate the presence of a CNS-specific antigen driven humoral immune response in the CSF compartment of AIE patients. It was shown by other groups that at the time of diagnosis, autoantibodies are always detectable in the CSF but not in the serum of 13% of AIE patients[120]. We presume that autoreactive B cell affinity maturation occurs inside the CNS compartment and some of the clonally related B cells migrate to the peripheral system to produce self-reactive antibodies. However, we currently have no data to support this hypothesis and further experimental effort is being made to identify the autoantibody producing CSF cePc in the peripheral blood compartment of the same patients. The pathogenic role of these antibodies is supported by the response of clinical symptoms to immunotherapy and the correlation between antibody titers and neurological outcome. It has been reported that immunoglobulins isolated from CSF and sera of patients with anti-NMDA receptor encephalitis can reduce NMDA receptor clusters on hippocampal neurons *in vitro*.[55] In another study, intra-ventricular injection of patients' CSF into mice leads to memory loss and depression.[123] Since all these studies have been carried out with autoantibodies recovered in the form of impure and heterogeneous mixtures from the CSF and/or serum of affected patients, it is not yet clear whether a single or a group of autoantibodies is responsible for the disease, and clearly impairs their further concise characterization.

Having patient derived anti-neuronal autoantibodies in recombinant monoclonal form may facilitate the characterization of their precise epitope specificity and functional properties and help to understand the exact mechanism of their role in disease pathogenesis *in vitro* and *in vivo*. Some of the patient derived antineuronal rhuMAb could also be used to study their therapeutic usefulness in other neurological diseases, in which it may be beneficial e.g. to block NMDA receptor mediated excitotoxicity.

REFERENCES

1. Fairfax KA, Kallies A, Nutt SL, Tarlinton DM. Plasma cell development: from B-cell subsets to long-term survival niches. Semin Immunol. 2008; 20(1):49-58.
2. Nikoloudis D, Pitts JE, Saldanha JW. A complete, multi-level conformational clustering of antibody complementarity-determining regions. PeerJ. 2014 :e456.
3. Tanaka T, Rabbitts TH. Protocol for the selection of single-domain antibody fragments by third generation intracellular antibody capture. Nat Protoc. 2010; 5(1):67-92.
4. de Villartay JP, Fischer A, Durandy A. The mechanisms of immune diversification and their disorders. Nat Rev Immunol. 2003; 3(12):962-72.
5. Dalmau J, Tüzün E, Wu HY, et.al. Paraneoplastic anti-N-methyl-D-aspartate receptor encephalitis associated with ovarian teratoma. Ann Neurol. 2007; 61(1):25-36.
6. Gallardo E, Martínez-Hernández E, Titulaer MJ, Huijbers MG, et al. Cortactin autoantibodies in myasthenia gravis. Autoimmun Rev. 2014; 13(10):1003-1007.
7. Irani SR, Vincent A. The expanding spectrum of clinically-distinctive, immunotherapy-responsive autoimmune encephalopathies. Arq Neuropsiquiatr. 2012; 70(4):300-4.
8. Ciccoto G, Blaya M, Kelley RE. Stiff person syndrome. Neurol Clin. 2013; 31(1):319-28.
9. Wingerchuk DM, Weinshenker BG. Neuromyelitis optica (Devic's syndrome). Handb Clin Neurol. 2014; 122:581-99.
10. Renaudineau Y, Garaud S, Le Dantec C, Alonso-Ramirez R, Daridon C, Youinou P. Autoreactive B cells and epigenetics. Clin Rev Allergy Immunol. 2010; 39(1):85-94.
11. Zhang H, Zhou C, Wu L, Ni F, Zhu J, Jin T. Are onconeural antibodies a clinical phenomenology in paraneoplastic limbic encephalitis? Mediators Inflamm. 2013; 2013: 172986.
12. Vincent A, Bien CG, Irani SR, Waters P. Autoantibodies associated with diseases of the CNS: new developments and future challenges. Lancet Neurol 2011; 10:759-772.
13. Erlander MG, Tillakaratne NJ, Feldblum S, Patel N, Tobin AJ. Two genes encode distinct glutamate decarboxylases. Neuron. 1991; 7(1):91-100.
14. Georgieva Z, Parton M. Cerebellar ataxia and epilepsy with anti-GAD antibodies: treatment with IVIG and plasmapheresis. BMJ Case Rep. 2014 Jan 13;2014.
15. Bárová H, Perusicová J, Hill M, Sterzl I, Vondra K, Masek Z. Anti-GAD-positive patients with type 1 diabetes mellitus have higher prevalence of autoimmune thyroiditis than anti-GAD-negative patients with type 1 and type 2 diabetes mellitus. Physiol Res. 2004; 53(3):279-86.
16. Pasquale F. Finelli. Autoimmune Limbic Encephalitis With GAD Antibodies. Neurohospitalist. 2011; 1(4): 178–181.
17. Akman CI, Patterson MC, Rubinstein A, Herzog R. Limbic encephalitis associated with anti-GAD antibody and common variable immune deficiency. Dev Med Child Neurol. 2009; 51(7):563-7.
18. Boronat A, Sabater L, Saiz A, Dalmau J, Graus F. GABA(B) receptor antibodies in limbic encephalitis and anti-GAD-associated neurologic disorders. Neurology. 2011; 76(9):795-800.
19. Lai M, Hughes EG, Peng X, Zhou L, et.al. AMPA receptor antibodies in limbic encephalitis alter synaptic receptor location. Ann Neurol. 2009; 65(4):424-34.
20. Höftberger R, Titulaer MJ, Sabater L, et.al. Encephalitis and GABAB receptor antibodies: novel findings in a new case series of 20 patients. Neurology. 2013; 81(17):1500-6.
21. Tüzün E, Dalmau J. Limbic encephalitis and variants: classification, diagnosis and treatment. Neurologist. 2007; 13(5):261-71.

22. Buckley C, Oger J, Clover L, et al. Potassium channel antibodies in two patients with reversible limbic encephalitis. Ann Neurol. 2001; 50: 73–78.
23. Vincent A, Buckley C, Schott JM, et al. Potassium channel antibody-associated encephalopathy: a potentially immunotherapy-responsive form of limbic encephalitis. Brain. 2004; 127 (3): 701–712.
24. Thieben MJ, Lennon VA, Boeve BF, et al. Potentially reversible auto-immune limbic encephalitis with neuronal potassium channel antibody. Neurology. 2004; 62 (7): 1177–1182.
25. Schulte U, Thumfart JO, Klöcker N, et al. The epilepsy-linked Lgi1 protein assembles into presynaptic Kv1 channels and inhibits inactivation by Kvbeta1. Neuron. 2006; 49(5):697-706.
26. Poliak S, Gollan L, Martinez R, Custer A, et al. Caspr2, a new member of the neurexin superfamily, is localized at the juxtaparanodes of myelinated axons and associates with K+ channels. Neuron. 1999; 24(4):1037-47.
27. Traka M, Goutebroze L, Denisenko N, et al. Association of TAG-1 with Caspr2 is essential for the molecular organization of juxtaparanodal regions of myelinated fibers. J Cell Biol. 2003; 162(6):1161-72.
28. Fukata Y, Adesnik H, Iwanaga T, Bredt DS, Nicoll RA, Fukata M. Epilepsy-related ligand/receptor complex LGI1 and ADAM22 regulate synaptic transmission. Science. 2006; 313(5794):1792-5.
29. Fukata Y, Lovero KL, Iwanaga T, et al. Disruption of LGI1-linked synaptic complex causes abnormal synaptic transmission and epilepsy. Proc Natl Acad Sci U S A. 2010; 107(8):3799-804.
30. Lee R, Buckley C, Irani SR, Vincent A. Autoantibody testing in encephalopathies. Pract Neurol. 2012; 12(1):4-13.
31. Ohkawa T, Fukata Y, Yamasaki M, et al. Autoantibodies to epilepsy-related LGI1 in limbic encephalitis neutralize LGI1-ADAM22 interaction and reduce synaptic AMPA receptors. J Neurosci. 2013; 33(46):18161-74.
32. Shillito P, Molenaar PC, Vincent A, et al. Acquired neuromyotonia: evidence for autoantibodies directed against K+ channels of peripheral nerves. Ann Neurol. 1995; 38(5):714-22.
33. Liguori R, Vincent A, Clover L, et al. Morvan's syndrome: peripheral and central nervous system and cardiac involvement with antibodies to voltage-gated potassium channels. Brain. 2001; 124(Pt 12):2417-26.
34. Josephs KA, Silber MH, Fealey RD, Nippoldt TB, Auger RG, Vernino S. Neurophysiologic studies in Morvan syndrome. J Clin Neurophysiol. 2004; 21(6):440-5.
35. Irani SR, Michell AW, Lang B, et al. Faciobrachial dystonic seizures precede Lgi1 antibody limbic encephalitis. Ann Neurol. 2011; 69(5):892-900.
36. Tan KM, Lennon VA, Klein CJ, Boeve BF, Pittock SJ Clinical spectrum of voltage-gated potassium channel autoimmunity. Neurology. 2008; 70(20):1883-90.
37. Pakozdy A, Halasz P, Klang A, Bauer J, et al. Suspected limbic encephalitis and seizure in cats associated with voltage-gated potassium channel (VGKC) complex antibody. J Vet Intern Med. 2013; 27(1):212-4.
38. Lai M, Huijbers MG, Lancaster E, Graus F, Bataller L, Balice-Gordon R, Cowell JK, Dalmau J. Investigation of LGI1 as the antigen in limbic encephalitis previously attributed to potassium channels: a case series. Lancet Neurol. 2010; 9(8):776-85.

39. Irani SR, Alexander S, Waters P, et al. Antibodies to Kv1 potassium channel-complex proteins leucine-rich, glioma inactivated 1 protein and contactin-associated protein-2 in limbic encephalitis, Morvan's syndrome and acquired neuromyotonia. Brain. 2010; 133(9):2734-48.
40. Lancaster E, Huijbers MG, Bar V, et al. Investigations of caspr2, an autoantigen of encephalitis and neuromyotonia. Ann Neurol. 2011; 69(2):303–311
41. Lee CH, Lin JJ, Lin KJ, Chang BL, Hsieh HY, Chen WH, Lin KL, Fung HC, Wu T. Caspr2 antibody limbic encephalitis is associated with Hashimoto thyroiditis and thymoma. J Neurol Sci. 2014; 341(1-2):36-40.
42. Loukaides P, Schiza N, Pettingill P, Palazis L, Vounou E, Vincent A, Kleopa KA. Morvan's syndrome associated with antibodies to multiple components of the voltage-gated potassium channel complex. J Neurol Sci. 2012; 312(1-2):52-6.
43. Lalic T, Pettingill P, Vincent A, Capogna M. Human limbic encephalitis serum enhances hippocampal mossy fiber-CA3 pyramidal cell synaptic transmission. Epilepsia. 2011; 52(1):121-31.
44. Morante-Redolat JM, Gorostidi-Pagola A, et al. Mutations in the LGI1/Epitempin gene on 10q24 cause autosomal dominant lateral temporal epilepsy. Hum Mol Genet. 2002; 11(9):1119-28.
45. Chabrol E, Navarro V, Provenzano G, et al. Electroclinical characterization of epileptic seizures in leucine-rich, glioma-inactivated 1-deficient mice. Brain. 2010; 133(9):2749-62.
46. Strauss KA, Puffenberger EG, Huentelman MJ, Gottlieb S, Dobrin SE, Parod JM, Stephan DA, Morton DH.Recessive symptomatic focal epilepsy and mutant contactin-associated protein-like 2. N Engl J Med. 2006; 354(13):1370-7.
47. Li F, Tsien JZ. Memory and the NMDA receptors. N Engl J Med. 2009; 361(3):302-3.
48. Karakas E and Furukawa H. Crystal structure of a heterotetrameric NMDA receptor ion channel. Science. 2014; 344(6187):992-7.
49. Stys PK, You H, Zamponi GW. Copper-dependent regulation of NMDA receptors by cellular prion protein: implications for neurodegenerative disorders. J Physiol. 2012; 590(Pt 6):1357-68.
50. Kleckner NW, Dingledine R. Requirement for glycine in activation of NMDA-receptors expressed in Xenopus oocytes. Science. 1988; 241(4867):835-7.
51. Dingledine R, Borges K, Bowie D, Traynelis SF. The glutamate receptor ion channels. Pharmacol Rev. 1999; 51(1):7-61.
52. Coyle JT. Glutamate and schizophrenia: beyond the dopamine hypothesis. Cell Mol Neurobiol 2006; 26: 365–84.
53. Waxman EA, Lynch DR. N-methyl-D-aspartate receptor subtypes: multiple roles in excitotoxicity and neurological disease. Neuroscientist 2005; 11: 37–49.
54. Lau CG, Zukin RS. NMDA receptor traffi cking in synaptic plasticity and neuropsychiatric disorders. Nat Rev Neurosci 2007; 8: 413–26.
55. Dalmau J, Gleichman AJ, Hughes EG, Rossi JE, Peng X, Lai M, Dessain SK, Rosenfeld MR, Balice-Gordon R, Lynch DR. Anti-NMDA-receptor encephalitis: case series and analysis of the effects of antibodies. Lancet Neurol. 2008; 7(12):1091-8.
56. Wickström R, Fowler A, Cooray G, Karlsson-Parra A, Grillner P. Viral triggering of anti-NMDA receptor encephalitis in a child - An important cause for disease relapse. Eur J Paediatr Neurol. 2014; 18(4):543-6.

57. Mann A, Machado NM, Liu N, Mazin AH, Silver K, Afzal KI. A multidisciplinary approach to the treatment of anti-NMDA-receptor antibody encephalitis: a case and review of the literature. J Neuropsychiatry Clin Neurosci. 2012; 24(2):247-54.
58. Le Moigno L, Ternant D, Paintaud G, Thibault G, Cloarec S, Tardieu M, Lagrue E, Castelnau P. [N-methyl-D-aspartate receptor antibody encephalitis: value of immunomodulatory therapy]. Arch Pediatr. 2014; 21(6):620-3.
59. DeSena AD, Greenberg BM, Graves D. "Light Switch" Mental Status Changes and Irritable Insomnia are Two Particularly Salient Features of Anti-NMDA Receptor Antibody Encephalitis. Pediatr Neurol. 2014; 51(1):151-3.
60. Moscato EH, Peng X, Jain A, Parsons TD, Dalmau J, Balice-Gordon RJ. Acute mechanisms underlying antibody effects in anti-NMDA receptor encephalitis. Ann Neurol. 2014; 76(1):108-19.
61. Gilbert GJ. Herpes simplex virus-1 encephalitis can trigger anti-NMDA receptor encephalitis: case report. Neurology. 2014; 82(22):2041.
62. Ryan TJ, Emes RD, Grant SG, Komiyama NH. Evolution of NMDA receptor cytoplasmic interaction domains: implications for organisation of synaptic signalling complexes. BMC Neurosci. 2008; 9:6.
63. Kemp, J. A. & McKernan, R. M. NMDA receptors as drug targets. Nature Neurosci. 2002; 5:1039–1042.
64. Tüzün E, Zhou L, Baehring JM, Bannykh S, Rosenfeld MR, Dalmau J. Evidence for antibody-mediated pathogenesis in anti-NMDAR encephalitis associated with ovarian teratoma. Acta Neuropathol 2009; 118:737-43
65. Titulaer MJ, McCracken L, et al. Treatment and prognostic factors for long-term outcome in patients with anti-NMDA receptor encephalitis: an observational cohort study. Lancet Neurol. 2013; 12(2):157-65.
66. Hollmann M, Heinemann S. Cloned glutamate receptors. Annu Rev Neurosci. 1994; 17:31-108.
67. Bassani S, Valnegri P, Beretta F, Passafaro M. The GLUR2 subunit of AMPA receptors: synaptic role. Neuroscience. 2009; 158(1):55-61.
68. Whitlock JR, Heynen AJ, Shuler MG, Bear MF. Learning induces long-term potentiation in the hippocampus. Science. 2006; 313(5790): 1093–7.
69. Keinänen K, Wisden W, Sommer B, Werner P, Herb A, Verdoorn TA, Sakmann B, Seeburg PH. A family of AMPA-selective glutamate receptors. Science. 1990; 249(4968):556-60.
70. Monyer H, Seeburg PH, Wisden W. Glutamate-operated channels: developmentally early and mature forms arise by alternative splicing.Neuron. 1991; 6(5):799-810.
71. Rogawski MA. AMPA receptors as a molecular target in epilepsy therapy. Acta Neurol Scand Suppl. 2013; (197):9-18.
72. Graus F, Boronat A, XifróX, Boix M, Svigelj V, García A, Palomino A, Sabater L, Alberch J, Saiz A. The expanding clinical profile of anti-AMPA receptor encephalitis. Neurology. 2010; 74(10):857.
73. Goldberg-Stern H, Ganor Y, Cohen R, Pollak L, Teichberg V, Levite M. Glutamate receptor antibodies directed against AMPA receptors subunit 3 peptide B (GluR3B) associate with some cognitive/psychiatric/behavioral abnormalities in epilepsy patients. Psychoneuroendocrinology. 2014; 40:221-31.

74. Spatola M, Stojanova V, Prior JO, Dalmau J, Rossetti AO. Serial brain ^{18}FDG-PET in anti-AMPA receptor limbic encephalitis. J Neuroimmunol. 2014; 271(1-2):53-5.
75. Wei YC, Liu CH, Lin JJ, Lin KJ, Huang KL, Lee TH, Chang YJ, Peng TI, Lin KL, Chang TY, Chang CH, Kuo HC, Chang KH, Cheng MY, Huang CC. Rapid progression and brain atrophy in anti-AMPA receptor encephalitis. J Neuroimmunol. 2013; 261(1-2):129-33.
76. Ganor Y, Goldberg-Stern H, Cohen R, Teichberg V, Levite M. Glutamate receptor antibodies directed against AMPA receptors subunit 3 peptide B (GluR3B) can be produced in DBA/2J mice, lower seizure threshold and induce abnormal behavior. Psychoneuroendocrinology. 2014; 42:106-17.
77. Lynch JW: Molecular structure and function of the glycine receptor chloride channel. Physiological reviews: 2004, 84 (4): 1051–95.
78. Legendre, P. The glycinergic inhibitory synapse. Cell. Mol. Life Sci. 2001, 58, 760–793.
79. Grenningloh G, Pribilla I, Prior P, Multhaup G, Beyreuther K, Taleb O, Betz H. Cloning and expression of the 58 kd beta subunit of the inhibitory glycine receptor. Neuron. 1990; 4(6):963-70.
80. Grenningloh, G., Schmieden, V., Schofield, P. R., Seeburg, P. H., Siddique, T., Mohandas, T. K., Becker, C. M., and Betz, H. α subunit variants of the human glycine receptor: primary structures, functional expression and chromosomal localization of the corresponding genes. EMBO J. 1990; 9(3):771-6.
81. Kuhse, J., Schmieden, V., and Betz, H. Identification and functional expression of a novel ligand binding subunit of the inhibitory glycine receptor. J. Biol. Chem. 1990; 265, 22317–22320.
82. Grudzinska, J., Schemm, R., Haeger, S., Nicke, A., Schmalzing, G., Betz, H., and Laube, B. The β subunit determines the ligand binding properties of synaptic glycine receptors. Neuron: 2005; 45, 727–739.
83. Yang, Z., Taran, E., Webb, T. I., and Lynch, J. W. Stoichiometry and subunit arrangement of α1β glycine receptors as determined by atomic force microscopy. Biochemistry: 2012; 51, 5229–5231.
84. Dutertre S, Becker CM, Betz H. Inhibitory glycine receptors: an update. J Biol Chem. 2012; 287(48):40216-23.
85. Bode A, Lynch JW. The impact of human hyperekplexia mutations on glycine receptor structure and function. Mol Brain. 2014; 7:2.
86. Hutchinson M, Waters O, McHugh J, et al. Progressive encephalomyelitis, rigidity and myoclonus: a novel glycine receptor antibody. Neurology 2008; 71:1291-2.
87. Carvajal-González A, Leite MI, Waters P, et al. Glycine receptor antibodies in PERM and related syndromes: characteristics, clinical features and outcomes. Brain. 2014; 137(Pt 8):2178-92.
88. Clerinx K, Breban T, Schrooten M, Leite MI, Vincent A, Verschakelen J, et al. Progressive encephalomyelitis with rigidity and myoclonus: resolution after thymectomy. Neurology. 2011; 76: 303–4.
89. Damasio J, Leite MI, Coutinho E, Waters P, Woodhall M, Santos MA, et al. Progressive encephalomyelitis with rigidity and myoclonus: the first pediatric case with glycine receptor antibodies. JAMA Neurol. 2013; 70: 498–501.

90. Bourke D, Roxburgh R, Vincent A, Cleland J, Jeffery O, Dugan N, et al. Hypoventilation in glycine-receptor antibody related progressive encephalomyelitis, rigidity and myoclonus. J Clin Neurosci. 2014; 21: 876–8.
91. Alexopoulos H, Akrivou S, Dalakas MC. Glycine receptor antibodies in stiff-person syndrome and other GAD-positive CNS disorders. Neurology. 2013; 81(22):1962-4.
92. McKeon A, Martinez-Hernandez E, Lancaster E, Matsumoto JY, Harvey RJ, McEvoy KM, Pittock SJ, Lennon VA, Dalmau J. Glycine receptor autoimmune spectrum with stiff-man syndrome phenotype. JAMA Neurol. 2013; 70(1):44-50.
93. Clardy SL, Lennon VA, Dalmau J, Pittock SJ, Jones HR Jr, Renaud DL, Harper CM Jr, Matsumoto JY, McKeon A. Childhood onset of stiff-man syndrome. JAMA Neurol. 2013; 70(12):1531-6.
94. Turner MR, Irani SR, Leite MI, Nithi K, Vincent A, Ansorge O. Progressive encephalomyelitis with rigidity and myoclonus: glycine and NMDA receptor antibodies. Neurology 2011; 77: 439–43.
95. Stern WM, Howard R, Chalmers RM, Woodhall MR, Waters P, Vincent A, et al. Glycine receptor antibody mediated Progressive Encephalomyelitis with Rigidity and Myoclonus (PERM): a rare but treatable neurological syndrome. Pract Neurol 2014; 14: 123–7.
96. Ohkawa T, Satake S, Yokoi N, Miyazaki Y, Ohshita T, Sobue G, Takashima H, Watanabe O, Fukata Y, Fukata M. Identification and Characterization of GABAA Receptor Autoantibodies in Autoimmune Encephalitis. J Neurosci. 2014; 34(24):8151-63.
97. Lancaster E, Lai M, Peng X, Hughes E, Constantinescu R, et, al. Antibodies to the GABA(B) receptor in limbic encephalitis with seizures: case series and characterisation of the antigen. Lancet Neurol. 2010; 9(1):67-76.
98. Macdonald RL, Olsen RW. GABAA receptor channels. Annu Rev Neurosci. 1994; 17:569–602.
99. Jacob TC, Moss SJ, Jurd R. GABAA receptor trafficking and its role in the dynamic modulation of neuronal inhibition. Nat Rev Neurosci. 2008; 9:331–343.
100. Rudolph U, Knoflach F. Beyond classical benzodiazepines: novel therapeutic potential of GABAA receptor subtypes. Nat Rev Drug Discov. 2011; 10:685– 697.
101. Macdonald RL, Kang JQ, Gallagher MJ. Mutations in GABAA receptor subunits associated with genetic epilepsies. J Physiol.2010; 588:1861–1869.
102. DeLorey TM, Handforth A, Anagnostaras SG, Homanics GE, Minassian BA, Asatourian A, Fanselow MS, Delgado-Escueta A, Ellison GD, Olsen RW. Mice lacking the beta3 subunit of the GABAA receptor have the epilepsy phenotype and many of the behavioral characteristics of Angelman syndrome. J Neurosci. 1998; 18:8505– 8514.
103. Kaupmann K, Malitschek B, Schuler V, Heid J, Froestl W, Beck P, Mosbacher J, Bischoff S, Kulik A, Shigemoto R, Karschin A, Bettler B. GABA(B)-receptor subtypes assemble into functional heteromeric complexes.Nature. 1998; 396(6712):683-7.
104. Marshall FH, Jones KA, Kaupmann K, Bettler B.GABAB receptors - the first 7TM heterodimers. Trends Pharmacol Sci. 1999; 20(10):396-9.
105. Kaupmann K, Schuler V, Mosbacher J, Bischoff S, Bittiger H, Heid J, Froestl W, Leonhard S, Pfaff T, Karschin A, Bettler B. Human γ-aminobutyric acid type B receptors are differentially expressed and regulate inwardly rectifying K^+ channels. Proc Natl Acad Sci U S A. 1998; 95(25):14991-6.

106. Bowery NG, Enna SJ. gamma-aminobutyric acid(B) receptors: first of the functional metabotropic heterodimers. J Pharmacol Exp Ther. 2000; 292(1):2-7.
107. Lancaster E, Martinez-Hernandez E, Titulaer MJ, Boulos M, et al. Antibodies to metabotropic glutamate receptor 5 in the Ophelia syndrome. Neurology. 2011; 77:1698–1701.
108. von Büdingen HC, Gulati M, Kuenzle S, Fischer K, Rupprecht TA, Goebels N. Clonally expanded plasma cells in the cerebrospinal fluid of patients with central nervous system autoimmune demyelination produce "oligoclonal bands". J Neuroimmunol. 2010; 218(1-2):134-9.
109. Obermeier B, Mentele R, Malotka J, Kellermann J, Kümpfel T, Wekerle H, Lottspeich F, Hohlfeld R, Dornmair K. Matching of oligoclonal immunoglobulin transcriptomes and proteomes of cerebrospinal fluid in multiple sclerosis. Nat Med. 2008 Jun;14(6):688-93. doi: 10.1038/nm1714. Epub 2008 May 18.
110. Owens GP, Winges KM, Ritchie AM, Edwards S, Burgoon MP, Lehnhoff L, Nielsen K, Corboy J, Gilden DH, Bennett JL. VH4 gene segments dominate the intrathecal humoral immune response in multiple sclerosis. J Immunol. 2007; 179(9):6343-51.
111. Fraser NL, Rowley G, Field M, Stott DI. The VH gene repertoire of splenic B cells and somatic hypermutation in systemic lupus erythematosus. Arthritis Res Ther. 2003; 5(2):R114-21.
112. Dalmau J, Rosenfeld MR. Autoimmune encephalitis update. Neuro Oncol. 2014; 16(6):771-8.
113. Tiller T, Meffre E, Yurasov S, Tsuiji M, Nussenzweig MC, Wardemann H. Efficient generation of monoclonal antibodies from single human B cells by single cell RT-PCR and expression vector cloning. J Immunol Methods. 2008; 329(1-2):112-24.
114. Kabat, EA.; Wu, TT.; Perry, HM.; Gottesman, KS.; Foeller, C. Sequences of proteins of immunological Interest. NIH publication; 1991.
115. Saitou N, Nei M. The neighbor-joining method: a new method for reconstructing phylogenetic trees. Mol Biol Evol. 1987; 4(4):406-25.
116. Hillis DM, Bull JJ, White ME, Badgett MR, Molineux IJ. Experimental phylogenetics: generation of a known phylogeny. Science. 1992; 255(5044):589-92.
117. http://www.euroimmun.de/index.php?id=1&L=1
118. Florance NR, Davis RL, Lam C, Szperka C, Zhou L, Ahmad S, Campen CJ, Moss H, Peter N, Gleichman AJ, Glaser CA, Lynch DR, Rosenfeld MR, Dalmau J. Anti-N-methyl-D-aspartate receptor (NMDAR) encephalitis in children and adolescents. Ann Neurol. 2009; 66(1):11-8.
119. Moscato EH, Jain A, Peng X, Hughes EG, Dalmau J, Balice-Gordon RJ. Mechanisms underlying autoimmune synaptic encephalitis leading to disorders of memory, behavior and cognition: insights from molecular, cellular and synaptic studies. Eur J Neurosci. 2010; 32(2):298-309.
120. Gresa-Arribas N, Titulaer MJ, Torrents A, et al. Antibody titres at diagnosis and during follow-up of anti-NMDA receptor encephalitis: a retrospective study. Lancet Neurol. 2014 Feb;13(2):167-77.
121. Ishida K, Mitoma H, Mizusawa H. Reversibility of cerebellar GABAergic synapse impairment induced by anti-glutamic acid decarboxylase autoantibodies. J Neurol Sci. 2008 Aug 15;271(1-2):186-90.
122. Burton AR, Vincent E, Arnold PY, et al. On the pathogenicity of autoantigen-specific T-cell receptors. Diabetes. 2008; 57(5):1321-30.

123. Francesco M, Cuesta$_7$ GJ, Leypoldt F et al. From Behavior To Synapse: A Murine Model Of Passive Transfer Of Antibodies From Patients With Anti-NMDAR Encephalitis (S63.007). Neurology April 8, 2014 vol. 82 no. 10 Supplement S63.007.
124. Raymond C, Tom R, Perret S, Moussouami P, et al. A simplified polyethylenimine-mediated transfection process for large-scale and high-throughput applications. Methods. 2011; 55(1):44-51.
125. http://www.invivogen.com/antibody-generation
126. Freund NT, Enshell-Seijffers D, Gershoni JM. Phage display selection, analysis, and prediction of B cell epitopes. Curr Protoc Immunol. 2009 Aug;Chapter 9:Unit 9.8.
127. Owens GP, Ritchie AM, Burgoon MP, Williamson RA, Corboy JR, Gilden DH. Single-cell repertoire analysis demonstrates that clonal expansion is a prominent feature of the B cell response in multiple sclerosis cerebrospinal fluid. J Immunol. 2003; 171(5):2725-33.
128. Stephenson FA. Structure and trafficking of NMDA and GABAA receptors. Biochem Soc Trans. 2006 Nov;34(Pt 5):877-81.
129. Tian N, Petersen C, Kash S, Baekkeskov S, Copenhagen D, Nicoll R. The role of the synthetic enzyme GAD65 in the control of neuronal gamma-aminobutyric acid release. Proc Natl Acad Sci U S A. 1999 Oct 26;96(22):12911-6.
130. Melcher T, Geiger JR, Jonas P, Monyer H. Analysis of molecular determinants in native AMPA receptors. Neurochem Int. 1996 Feb;28(2):141-4.

APPENDIX

ABBREVIATIONS

AIE	Autoimmune encephalitis
AMPAR	α-Amino-3-hydroxy-5-methyl-4-isoxazolepropionic acid receptor
CASPR2	Contactin-associated protein-like 2
CDR	Complementarity determining region
cePc	Clonally expanded plasma cells/plasmablasts
CNS	Central nervous system
CSF	Cerebrospinal fluid
E.coli	Escherichia coli
FACS	Fluorescence activated cell sorting
GABAR	Gamma-aminobutyric acid receptor
GAD_{65}	Glutamic acid decarboxylase
GlyR	Glycine receptor
ICC	Immunocytochemistry
Ig	Immunoglobulin
IPs	Immunoprecipitations
LGI1	Leucine-rich glioma inactivated protein 1
mGluR	metabotropic glutamate receptors
MOG	Myelin oligodendrocyte glycoprotein
NMDAR	*N*-Methyl-D-aspartic acid receptor
Pg.	Page number
rhuMAb	Recombinant human monoclonal antibodies
RT-PCR	Reverse transcriptase-polymerase chain reaction

ACKNOWLEDGEMENTS

My first thanks go to Prof. Dr. Norbert Goebels, for allowing me to pursue my thesis in the exciting new field of autoimmune encephalitis syndromes. His continuous support and interest was fundamental to the progress of my work. I appreciated the freedom and trust I received from him as it helped me to become self-motivated and independent.

I am also very grateful to Prof. Dr. Dieter Willbold, for being my second research supervisor.

I am indeed indebted and extend my deep sense of gratitude to all the patients who provided their valuable CSF and blood samples for my research work. My special thanks go to Mrs. Katharina Raba, for her help to collect single CSF-cell by FACS at Core Flow Cytometry Facility. I would like to thank Dr. Fatih Demir for his help with the immunoprecipitation experiments and also his valuable suggestions during the writing of my thesis.

I am very much thankful to my research colleagues Dr. Meike Winter; Ms. Christine Baksmeier; Ms. Julia Steckel; Mr. Armin Scheffler; Mr. Jason Cline and Mr. Sumanta Barman and to all other colleagues and friends at the Life Science Center, for their help and valuable suggestions.

I specially want to thank my parents and other family members for their support.

DECLARATION/ERKLÄRUNG

Hiermit erkläre ich, die vorliegende Arbeit selbstständig und ohne unerlaubte Hilfe verfasst und die verwendeten Quellen kenntlich gemacht zu haben. Diese Dissertation wurde bei keiner anderen Institution in dieser oder ähnlicher Form bisher eingereicht und es wurden keine erfolglosen Promotionsversuche unternommen.

Manish Malviya

Name:	Manish Malviya
Date of Birth:	2nd January 1983
Place of Birth:	Bhadohi, UP, India
Address in India:	Girdharpur, Gyanpur, Sant Ravidas Nagar Bhadohi- 221304, Utter Pradesh (Phone: +91-9415625149)
Address in Germany:	Moorenstrase-5, Geb.14.96, Zi.006, Düsseldorf-40225
Mobile:	+49-15751032364
Emails:	malviya.manish@gmail.com manish.malviya@med.uni-duesseldorf.de

EDUCATION

2011-2014	PhD theses AG Prof. Dr. Med. Norbert Goebels Department of Neurology, Heinrich Heine University, Düsseldorf
2009-2010	Research Assistant AG Prof. Dr. Jochen Walter Molecular Cell Biology, Department of Neurology, Sigmund-Freud-Str. 25, Bonn-53105, Germany
2005-2009	Research Assistant Prof. Subhash M. Nadgir, Department of Neurochemistry, National Institute of Mental Health and Neurosciences, Bangalore - 560029, India
2004-2005	Trainee Scientist in Bioinformatics Jubilant Biosys Limited, Bangalore. 2004-2005
2002-2004	Master of Science (M.Sc.) in Biochemistry, Banaras Hindu University, UP, India
1999-2004	Bachelor of Science (B.Sc.) in Chemistry, Zoology and Botany Veer Bahadur Singh Purvanchal University, Jaunpur, UP, India

1997-1999	Intermediate (12th Class) in Biology, Physics, Chemistry, English and Hindi Board of High school and Intermediate Education, UP, India
1997	High School (10th Class) in Biology, Mathematics, Science, Social science, English and Hindi Board of High school and Intermediate Education, UP, India

PUBLICATIONS

Manish Malviya, Kumar YC, Mythri RB, Venkateshappa C, Subhash MN, Rangappa KS. Muscarinic receptor 1 agonist activity of novel N-aryl carboxamide substituted 3-morpholino arecoline derivatives in Alzheimer's presenile dementia models. Bioorg Med Chem. 2009 Aug 1;17(15):5526-34.

Manish Malviya, Kumar YC, Asha D, Chandra JN, Subhash MN, Rangappa KS. Muscarinic receptor 1 agonist activity of novel N-arylthioureas substituted 3-morpholino arecoline derivatives in Alzheimer's presenile dementia models. Bioorg Med Chem. 2008 Aug 1;16(15):7095-101.

Nadgir SM, **Manish Malviya**. In vivo effect of antidepressants on [3H]paroxetine binding to serotonin transporters in rat brain. Neurochem Res. 2008 Nov;33(11):2250-6.

Chandra JN, **Manish Malviya**, Sadashiva CT, Subhash MN, Rangappa KS. Effect of novel arecoline thiazolidinones as muscarinic receptor 1 agonist in Alzheimer's dementia models. Neurochem Int. 2008 Feb;52(3):376-83.

Kumar YC, **Manish Malviya**, Chandra JN, Sadashiva CT, Kumar CS, Prasad SB, Prasanna DS, Subhash MN, Rangappa KS. Effect of novel N-aryl sulfonamide substituted 3-morpholino arecoline derivatives as muscarinic receptor 1 agonists in Alzheimer's dementia models. Bioorg Med Chem. 2008 May 1;16(9):5157-63.

Girisha HR, Narendra Sharath Chandra JN, Boppana S, **Manish Malviya**, Sadashiva CT, Rangappa KS. Active site directed docking studies: synthesis and pharmacological evaluation of cis-2,6-dimethyl piperidine sulfonamides as inhibitors of acetylcholinesterase. Eur J Med Chem. 2009 Oct;44(10):4057-62.